



# MARCH5 promotes STING pathway activation by suppressing polymer formation of oxidized STING

Kyungpyo Son<sup>†</sup>, Seokhwan Jeong<sup>†</sup> , Eunchong Eom<sup>†</sup>, Dohyeong Kwon<sup>‡</sup> & Suk-Jo Kang<sup>\*</sup> 

## Abstract

Stimulator of interferon genes (STING) is a core DNA sensing adaptor in innate immune signaling. STING activity is regulated by a variety of post-translational modifications (PTMs), including phosphorylation, ubiquitination, sumoylation, palmitoylation, and oxidation, as well as the balance between active and inactive polymer formation. It remains unclear, though, how different PTMs and higher order structures cooperate to regulate STING activity. Here, we report that the mitochondrial ubiquitin ligase MARCH5 (Membrane Associated Ring-CH-type Finger 5, also known as MITOL) ubiquitinates STING and enhances its activation. A long-term MARCH5 deficiency, in contrast, leads to the production of reactive oxygen species, which then facilitate the formation of inactive STING polymers by oxidizing mouse STING cysteine 205. We show that MARCH5-mediated ubiquitination of STING prevents the oxidation-induced STING polymer formation. Our findings highlight that MARCH5 balances STING ubiquitination and polymer formation and its control of STING activation is contingent on oxidative conditions.

**Keywords** MARCH5; oxidation; polymer; STING; ubiquitination

**Subject Categories** Immunology; Post-translational Modifications & Proteolysis; Signal Transduction

**DOI** 10.15252/embr.202357496 | Received 16 May 2023 | Revised 16 October 2023 | Accepted 18 October 2023 | Published online 2 November 2023

**EMBO Reports (2023) 24: e57496**

## Introduction

STING (stimulator of IFN genes, which is also known as TMEM173, MITA, MPYS, and ERIS) is an intracellular DNA sensing adaptor protein (Ishikawa & Barber, 2008; Zhong *et al.*, 2008; Sun *et al.*, 2009). STING has four transmembrane domains and is anchored as a dimer in the membrane of the endoplasmic reticulum (ER). STING binds cyclic GMP-AMP (cGAMP), which is the product of cGAS (cGAMP synthase) that recognizes intracellular DNA (Ablasser *et al.*, 2013; Sun *et al.*, 2013). Bacterial second messengers, cyclic di-nucleotides such as c-di-GMP and c-di-AMP, and synthetic chemicals 5,6-dimethylxanthenone-4-acetic acid (DMXAA), 10-carboxymethyl-

9-acridanone (CMA), and dimeric amidobenzimidazole (diABZI) can also activate STING (Barber, 2014; Decout *et al.*, 2021). Upon ligand binding, STING undergoes conformational changes (Ouyang *et al.*, 2012; Shang *et al.*, 2012; Shu *et al.*, 2012; Yin *et al.*, 2012), including an inward re-positioning of the ligand-binding domains (LBD) that seals the “lid” to ligand access (Huang *et al.*, 2012; Gao *et al.*, 2013; Zhang *et al.*, 2013; Kranzusch *et al.*, 2015) and a translocation of STING from the ER to the Golgi or perinuclear region (Ishikawa *et al.*, 2009; Saitoh *et al.*, 2009; Huang *et al.*, 2012; Ouyang *et al.*, 2012; Shang *et al.*, 2012; Shu *et al.*, 2012; Yin *et al.*, 2012; Dobbs *et al.*, 2015). Recently, cryo-electron microscopy (cryo-EM) analyses of STING revealed that cGAMP binding induces rotation of its LBDs and triggers its high-order oligomerization in a side-by-side arrangement of STING dimers (Ergun *et al.*, 2019; Shang *et al.*, 2019; Zhang *et al.*, 2019). STING oligomers function as a scaffold for the recruitment of TANK-binding kinase 1 (TBK1). TBK1 then phosphorylates STING at serine 366. The resulting phosphorylated STING recruits interferon regulatory factor 3 (IRF3), leading to its phosphorylation. Phosphorylated, active IRF3 then induces type-I interferon (IFN) (Tanaka & Chen, 2012; Liu *et al.*, 2015).

STING activity is regulated via a wide variety of post-translational modifications (PTMs). While phosphorylation of STING at serine 366 by TBK1 activates STING signaling (Liu *et al.*, 2015), phosphorylation of the same residue by UNC51-like kinase-1 (ULK1) induces STING degradation (Konno *et al.*, 2013). Numerous E3 ligases control STING function via various types of STING ubiquitination. For example, TRIM32 and TRIM56 interact with STING and ubiquitinate it via K63-linked ubiquitination, which facilitates STING dimerization and TBK1 activation (Tsuchida *et al.*, 2010; Zhang *et al.*, 2012). AMFR and INSIG facilitate TBK1 recruitment and activation via K27-linked polyubiquitination of STING (Wang *et al.*, 2014). MUL1, a mitochondria-localized E3 ligase, regulates STING activity via K63-linked ubiquitination (Ni *et al.*, 2017). In contrast, RNF5, TRIM29, and TRIM30 $\alpha$  reduce STING activation by promoting its degradation via K48-linked ubiquitination (Zhong *et al.*, 2009; Wang *et al.*, 2015; Xing *et al.*, 2017). There are also several deubiquitinases that regulate STING activation. CYLD stabilizes STING and enhances antiviral responses by removing K48-linked polyubiquitin chains from STING (Zhang *et al.*, 2018). USP20, which is recruited by USP18, also prevents STING degradation by deconjugating K48-linked polyubiquitin chains from STING (Zhang *et al.*, 2016). Similarly, USP49 inhibits

Department of Biological Sciences, Korea Advanced Institute of Science and Technology, Daejeon, Republic of Korea

\*Corresponding author. Tel: +82 42 350 2611; E-mail: [suk-jo.kang@kaist.ac.kr](mailto:suk-jo.kang@kaist.ac.kr)

<sup>†</sup>These authors contributed equally to this work

<sup>‡</sup>Present address: BOOSTIMMUNE, Inc, Seoul, Republic of Korea

STING oligomerization and TBK1 recruitment by removing K63-linked polyubiquitin chains from STING (Ye *et al.*, 2019). Recently, palmitoylation of STING at cysteines 88 and 91 was found to be essential for STING oligomerization in the Golgi (Mukai *et al.*, 2016). STING sumoylation at lysine 337 by TRIM38 promotes STING stability and activation, which is subsequently terminated when Smp2 catalyzes the desumoylation of STING (Hu *et al.*, 2016). Finally, several groups reported that reactive oxygen species (ROS) could suppress STING activity by its oxidation (Jin *et al.*, 2010; Tao *et al.*, 2020; Zamorano Cuervo *et al.*, 2021). The sheer number of STING PTMs implies a contextual and combinatorial fine-tuning of STING activity, but little is known about the relationships between the various STING PTMs.

Mitochondria are essential for not only regulating intracellular energy supply, metabolism, and apoptosis, but also as a signaling platform in innate immunity. Recently, we reported that mitochondrial dynamics are also critical regulators of STING signaling (Kwon *et al.*, 2017a, 2017b, 2018). The mitochondrial fusion mediator MFN1 enhances STING pathway activation (Kwon *et al.*, 2017a), whereas mitochondrial fission induced by the proton gradient disruptor CCCP or by the NLRP3 agonists ATP and nigericin inhibits STING pathway activation (Kwon *et al.*, 2017b, 2018). Furthermore, mitochondria-associated ER membranes (MAMs), which are sections of mitochondrial membrane in close enough proximity to ER membranes to allow chemical exchange (Missiroli *et al.*, 2018), can act as a hub for innate immune signaling (Weinberg *et al.*, 2015). RIG-I is recruited to MAMs to bind MAVS, which then enhances IFN- $\beta$  production (Horner *et al.*, 2011). NLRP3 inflammasomes are redistributed to MAMs after infection to induce inflammasome activation (Zhou *et al.*, 2011; Subramanian *et al.*, 2013). Intriguingly, STING is also localized to MAMs (Ishikawa *et al.*, 2009), but it remains unclear whether MAMs regulate STING activation.

Membrane-associated RING-CH-type finger (MARCH) proteins are E3 ubiquitin ligases that contain a C4HC3-type RING domain and that regulate diverse biological processes. These include aspects of immune responses, such as antigen presentation, cytokine signaling, and innate immune signaling (Bauer *et al.*, 2017; Lin *et al.*, 2019; Shiiba *et al.*, 2020). MARCH5 is the only MARCH family member that is localized to mitochondria, specifically to the outer mitochondrial membrane (OMM). MARCH5 reportedly inhibits mitochondrial fission through the ubiquitination and degradation of mitochondrial fission 1 (Fis1) (Yonashiro *et al.*, 2006), dynamin-related protein 1 (DRP1) (Nakamura *et al.*, 2006), and the DRP1 receptor Mid49 (Xu *et al.*, 2016). But, according to other reports, MARCH5 enhances mitochondrial fission (Karbowski *et al.*, 2007; Park & Cho, 2012). In addition to regulating mitochondrial dynamics, MARCH5 regulates MAM formation by ubiquitinating and activating MFN2 via K63-linked polyubiquitination (Sugiura *et al.*, 2013). Regarding its role in antiviral response regulation, MARCH5 enhances TLR7 signaling (Shi *et al.*, 2011) and suppresses RIG-I-like receptor (RLR) signaling (Yoo *et al.*, 2015). Still, MARCH5's role in the regulation of STING signaling remains unknown.

Here, we provide genetic and molecular evidence that MARCH5 suppresses ROS-mediated inhibition of STING signaling. We found a long-term MARCH5 deficiency increases intracellular ROS, which leads to STING oxidation, inactive polymer formation, and inhibition. We also found MARCH5 ubiquitinates STING and thereby prevents the ROS-induced inactive STING polymer formation.

## Results

### MARCH5 promotes STING-mediated type-I IFN production

We first examined the role of MARCH5 in STING pathway activation using a gain-of-function approach in which we co-transfected HEK293T cell lines with human STING-encoding plasmids and different amounts of human MARCH5-encoding plasmids. Additionally, HaCaT (human keratinocyte) and MEF (mouse embryonic fibroblast) cell lines were transfected with different amounts of plasmids encoding human and mouse MARCH5, respectively. We found that in all cell lines, increasing amounts of MARCH5 increased the production of IFN-stimulated gene 56 (ISG56), a target gene of IRF3 (Fig 1A, D and E). Increased MARCH5 also increased TBK1-mediated S366 phosphorylation of STING (p-STING) (Fig 1B and C). These results indicate that MARCH5 is sufficient to enhance STING pathway activation.

Next, we used MARCH5-deficient MEFs to determine whether MARCH5 is required for STING-mediated type-I IFN production. We measured ISG56 and IFN- $\beta$  mRNA production after stimulating the STING pathway by transfection with double-stranded (ds) DNA plasmids and cGAMP or by treatment with the STING agonists DMXAA and diABZI. We found *March5*<sup>-/-</sup> MEFs produced significantly less ISG56 and IFN- $\beta$  than wild-type (WT) MEFs (Fig 1F–I). These data suggest MARCH5 is both sufficient and necessary for inducing the STING-mediated type-I IFN response.

To verify that the defective STING pathway activation we observed in *March5*<sup>-/-</sup> MEFs is due to the absence of MARCH5 rather than something else, we performed a series of MARCH5 rescue experiments. First, we found that *March5*<sup>-/-</sup> MEFs transduced with a mouse *March5*-encoding virus produce more ISG56 in response to DMXAA than untransduced *March5*<sup>-/-</sup> MEFs (Fig 1J). When we tested whether the function of MARCH5 is conserved between mice and humans, we found that MARCH5 can promote STING-mediated ISG56 production regardless of species of MARCH5 and STING (Fig EV1A). Because we noticed that human MARCH5 is more stably expressed than mouse MARCH5 (Fig EV1B), we generated a human MARCH5-expressing *March5*<sup>-/-</sup> MEF stable cell line and confirmed rescue of STING pathway activation by again measuring ligand-induced ISG56 production (Fig 1K). These results demonstrate the role of MARCH5 as a positive regulator of the STING pathway, which is conserved between humans and mice.

### MARCH5 enhances STING phosphorylation but not translocation

To determine which step in the STING pathway is regulated by MARCH5, we measured IFN- $\beta$  promoter activity in WT and *March5*<sup>-/-</sup> MEFs transfected with plasmids encoding various innate immune signaling genes, as well as a construct encoding an IFN- $\beta$  luciferase reporter. While *March5*<sup>-/-</sup> MEFs did show reduced IFN- $\beta$  induction compared to WT in response to STING transfection, *March5*<sup>-/-</sup> MEFs and WT MEFs showed similar responses to TBK1 transfection (Fig 2A). This epistasis analysis indicated that MARCH5 regulates either TBK1 or some other molecule upstream from it. As previously reported (Seth *et al.*, 2005), *March5*<sup>-/-</sup> MEFs showed greater IFN- $\beta$  induction than WT in response to RIG-I or MAVS, which are both essential in RNA-sensing innate immunity. These

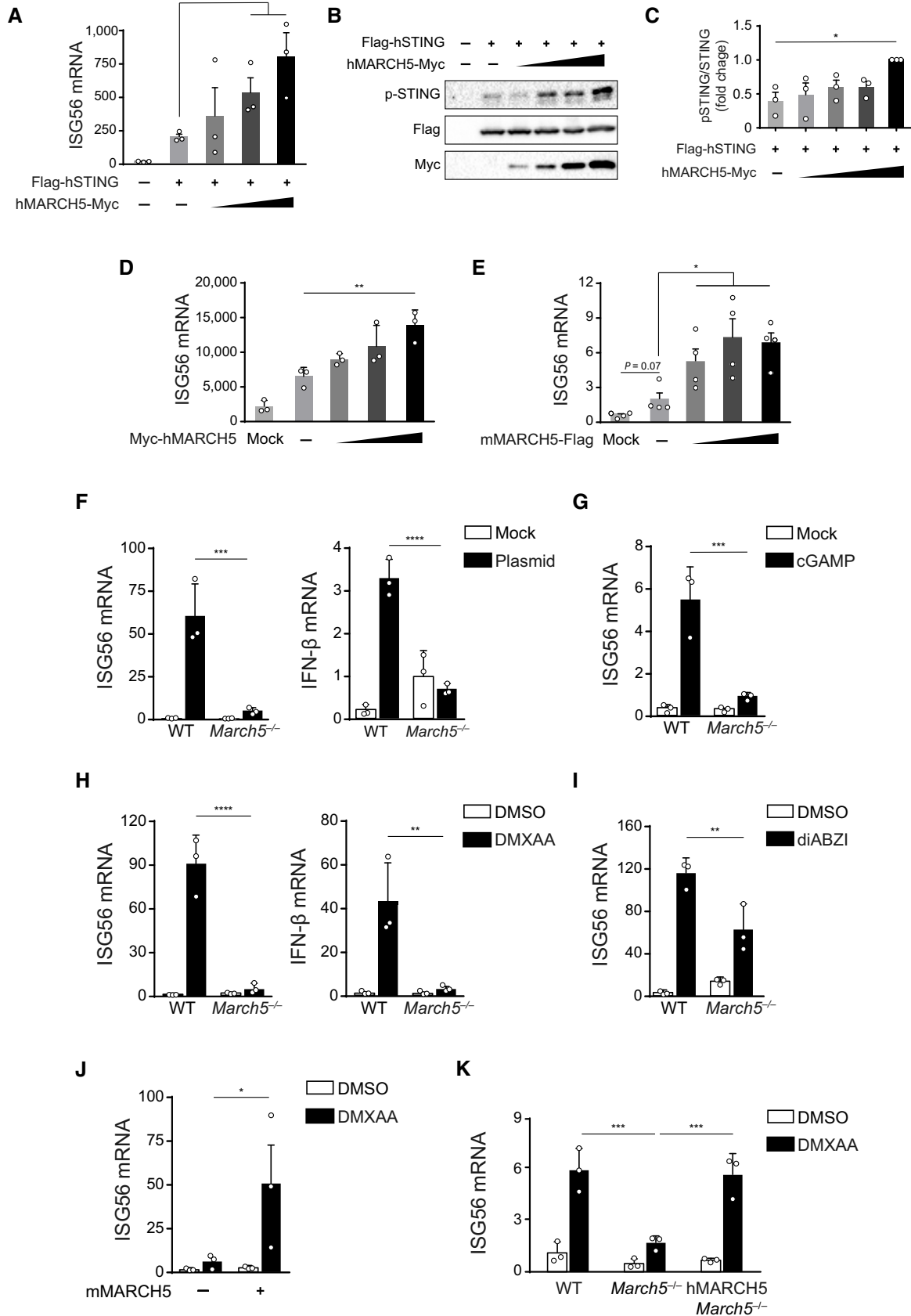


Figure 1.

**Figure 1. MARCH5 acts as a positive regulator of STING-mediated type-I IFN production.**

- A HEK293T cells were co-transfected with a plasmid encoding Flag-tagged human STING (Flag-hSTING) and different amounts (0.1, 0.2, 0.4  $\mu\text{g}$ ) of those encoding Myc-tagged human MARCH5 (hMARCH5-Myc). –, control plasmid alone. After 24 h, the induction of ISG56 mRNA was measured by RT-qPCR. Data are presented as mean  $\pm$  SEM ( $n = 3$ ).
- B HEK293T cells were co-transfected with a plasmid encoding Flag-tagged human STING (FLAG-hSTING) and different amounts (0.5, 1, 2, 4  $\mu\text{g}$ ) of those encoding Myc-tagged human MARCH5 (hMARCH5-Myc). –, control plasmid alone. After 24 h, cell lysates were resolved by SDS-PAGE. Total STING (Flag), phosphorylated STING (p-STING), and hMARCH5 (Myc) were detected by immunoblotting with the indicated antibodies.
- C Quantitation of the results of the three independent experiments that were representatively presented in (B). Phosphorylated STING (pSTING, normalized to total STING) levels at different amount of hMARCH5 were quantified and presented as mean  $\pm$  SEM ( $n = 3$ ).
- D HaCaT cells were transfected with different amounts (0.2, 0.4, 0.8  $\mu\text{g}$ ) of a plasmid encoding Myc-tagged human MARCH5 (hMARCH5-Myc). Mock, lipofectamine alone; –, control plasmid alone. After 24 h, the induction of ISG56 mRNA was measured by RT-qPCR. Data are presented as mean  $\pm$  SD ( $n = 3$ ).
- E WT MEFs were transfected with different amounts (0.1, 0.2, 0.4  $\mu\text{g}$ ) of a plasmid encoding Flag-tagged mouse MARCH5 (mMARCH5-Flag). Mock, lipofectamine alone; –, control plasmid alone. After 24 h, the induction of ISG56 mRNA was measured by RT-qPCR. Data are presented as mean  $\pm$  SEM ( $n = 4$ ).
- F–I Wild-type MEFs (WT) and *March5*<sup>-/-</sup> MEFs were transfected with lipofectamine alone (Mock) (F and G), plasmid DNA (5  $\mu\text{g}/\text{ml}$ ) for 6 h (F), or transfected with cGAMP (5  $\mu\text{g}/\text{ml}$ ) for 2 h (G), treated with DMSO (vehicle) or DMXAA (100  $\mu\text{g}/\text{ml}$ ) for 2 h (H), or treated with diABZI (10  $\mu\text{M}$ ) for 2 h (I). The induction of IFN- $\beta$  and ISG56 mRNAs was measured by RT-qPCR. Data are presented as mean  $\pm$  SD ( $n = 3$ ).
- J *March5*<sup>-/-</sup> MEFs were transduced with mouse MARCH5 (mMARCH5)-expressing viruses and treated with DMSO (vehicle) or DMXAA (100  $\mu\text{g}/\text{ml}$ ) for 2 h. The induction of ISG56 mRNA was measured by RT-qPCR. Data are presented as mean  $\pm$  SEM ( $n = 3$ ).
- K WT MEFs, *March5*<sup>-/-</sup> MEFs, and *March5*<sup>-/-</sup> MEFs stably expressing hMARCH5 (hMARCH5\_ *March5*<sup>-/-</sup>) were treated with DMSO (vehicle) or DMXAA (100  $\mu\text{g}/\text{ml}$ ) for 2 h, and the induction of ISG56 mRNA was measured by RT-qPCR. Data are presented as mean  $\pm$  SD ( $n = 3$ ).

Data information: The data are representative of at least two independent experiments.  $n$ , number of samples (biological replicates). Control vector was added to match the total plasmid amount (A–E). Statistical significance was analyzed by one-way ANOVA (A, C–E) or two-way ANOVA (F–K). \* $P < 0.05$ , \*\* $P < 0.01$ , \*\*\* $P < 0.001$ , \*\*\*\* $P < 0.0001$ .

Source data are available online for this figure.

data indicate that MARCH5 regulates the DNA- and RNA-sensing pathways differently.

Next, we used immunofluorescence to determine whether MARCH5 deficiency affects STING translocation, which occurs prior to TBK1-mediated STING phosphorylation. We found both WT and *March5*<sup>-/-</sup> MEFs that stably express Myc-tagged mouse STING showed similar levels of STING translocation to the Golgi, as visualized with an antibody against the cis-Golgi marker GM130, and measured by Pearson correlation coefficient for co-localization between STING and GM130 (Fig 2B and C). This suggests MARCH5 does not control STING translocation.

We next examined the activation of molecules downstream of STING over the course of 120 min following activation by DMXAA. We found that *March5*<sup>-/-</sup> MEFs showed reduced phosphorylation of STING, TBK1, and IRF3 compared to WT MEFs (Fig 2D), indicating that MARCH5 exerts its effect at the step immediately prior to STING activation. The quantitation results confirmed that the levels of pSTING and pIRF3 in *March5*<sup>-/-</sup> MEFs were significantly lower than those in WT MEFs (Fig 2E). Similarly, when we stimulated human MARCH5\_ *March5*<sup>-/-</sup> MEFs stably expressing human MARCH5 with DMXAA, they showed similar STING, TBK1, and IRF3 phosphorylation levels as WT MEFs (Fig 2F). The quantitation results confirmed that the levels of pSTING and pIRF3 in *March5*<sup>-/-</sup> MEFs were significantly lower than those in WT MEFs or human MARCH5-rescued *March5*<sup>-/-</sup> MEFs (Fig 2G). Collectively, these results suggest MARCH5 is a critical regulator of STING pathway activation at the step of STING phosphorylation.

**MARCH5 interacts with STING at the ER**

We then investigated whether and where MARCH5 interacts with STING to regulate STING signaling. When we overexpressed human STING and human MARCH5 in HEK293T cells and performed a co-immunoprecipitation, we were able to confirm the interaction between STING and MARCH5 (Fig 3A). Interestingly, STING also

interacted with the MARCH5 CS (C65/68S) mutant in which the cysteine residues of its catalytic domain are replaced with serine, blocking its E3 ubiquitin ligase activity (Fig 3A) (Yonashiro *et al*, 2006). This indicates MARCH5's E3 ligase activity is not required for its interaction with STING. Since STING overexpression can trigger STING activation, our interaction data in Fig 3A do not reveal whether STING and MARCH5 interact before or after STING activation. To determine which of these is the case, we generated HeLa cells that stably express Myc-tagged human STING and Flag-tagged wild-type human MARCH5. We then performed an *in situ* proximity ligation assay (PLA) with each tag. Although we observed significant levels of STING and MARCH5 ligation at the ER, probably at the MAM, prior to stimulation, plasmid transfection triggered a dramatic reduction in STING and MARCH5 ligation (Fig 3B). This indicates STING interacts with MARCH5 at steady state and dissociates from MARCH5 following activation.

To identify the domains responsible for the interaction between MARCH5 and STING, we generated various truncation mutants for both STING and MARCH5 and then subjected them to a series of co-immunoprecipitation analyses. STING protein can be divided into the N-terminus (NTD), which comprises four membrane-spanning helices, and the C-terminus (CTD), which includes both a ligand binding domain and a C-terminal tail (CTT) that binds TBK1 and IRF3 upon ligand stimulation (Huang *et al*, 2012; Ouyang *et al*, 2012; Shang *et al*, 2012; Shu *et al*, 2012; Yin *et al*, 2012). We first examined the interaction between MARCH5 and the STING truncation mutants by co-immunoprecipitation. We found that MARCH5 interacts with full-length WT STING and all the STING mutants (Fig 3C). Except the CTD mutant that is situated in the cytosol, all the other STING forms are localized in the ER (Fig EV2A). We measured the interaction between MARCH5 and WT or mutant STING in HEK293T cells by using a PLA assay. Our results demonstrate there is no difference in the extent of interaction between MARCH5 and all the STING forms (Fig EV2A). This suggests multiple points of contact in the interaction between MARCH5 and

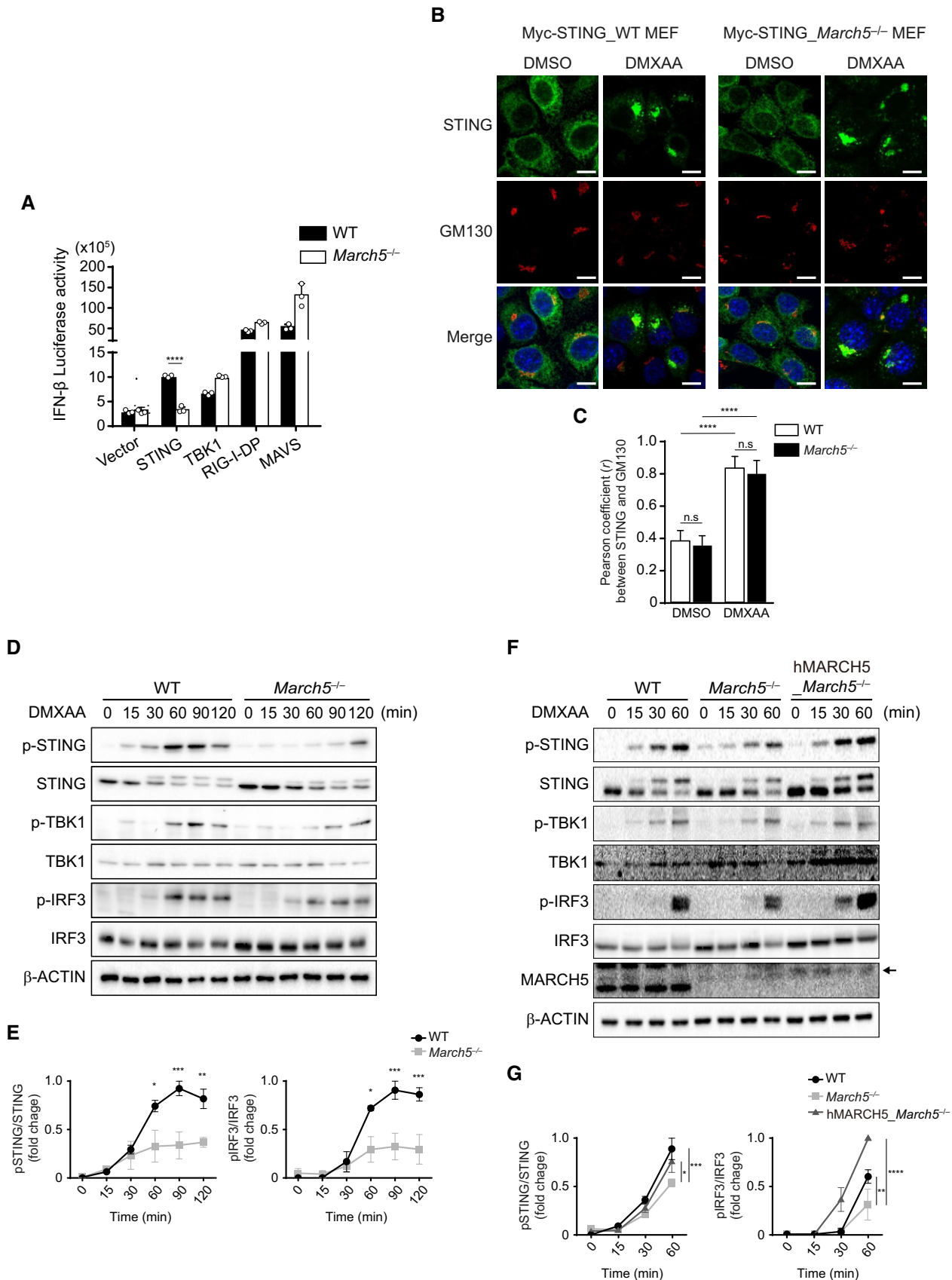


Figure 2.

**Figure 2. MARCH5 enhances STING phosphorylation.**

- A Luciferase assay of IFN- $\beta$  promoter activation in wild-type MEFs (WT) and *March5*<sup>-/-</sup> MEFs transfected with plasmids encoding STING, TBK1, a dominant positive form of RIG-I (RIG-I DP), or MAVS for 24 h. Data are presented as mean  $\pm$  SD ( $n = 3$ ).
- B, C Confocal micrographs showing the localization of STING in WT and *March5*<sup>-/-</sup> MEFs after stimulation. Myc-tagged mSTING was reconstituted in MEFs by retroviral transduction. The cells were stimulated with DMSO (vehicle) or DMXAA (100  $\mu$ g/ml) for 1 h and then STING, the *cis*-Golgi, and nuclei were visualized using anti-Myc (green), anti-GM130 (red) antibodies, and DAPI, respectively. Merged images are shown below. Magnification, 630 $\times$ . Scale bars: 10  $\mu$ m (B). Pearson correlation coefficients for STING and GM130 co-localization visualized in (B) are shown. Data are presented as mean  $\pm$  SD ( $n = 50$ ) (C).
- D–G WT and *March5*<sup>-/-</sup> MEFs (D and F) or *March5*<sup>-/-</sup> MEF cells stably expressing hMARCH5 (*hMARCH5\_March5*<sup>-/-</sup>) (F) were stimulated with DMXAA (100  $\mu$ g/ml) for the indicated times. Cell lysates were resolved by SDS–PAGE, and total STING, phosphorylated STING (p-STING), phosphorylated TBK1 (p-TBK1), total TBK1, phosphorylated IRF3 (p-IRF3), total IRF3, and  $\beta$ -ACTIN (loading control) or MARCH5 were detected via immunoblotting with the indicated antibodies. The black arrow shows Flag-tagged hMARCH5 expression (F). (E and G) Quantitation of the results of the three independent experiments that were representatively presented in (D and F), respectively. Phosphorylated STING (pSTING, normalized to total STING) and phosphorylated IRF3 (pIRF3, normalized to total IRF3) levels at different time points were quantified and presented as mean  $\pm$  SEM.

Data information: The data are representative of at least two independent experiments.  $n$ , number of samples (biological replicates). Statistical significance was analyzed by unpaired two-tail Student's  $t$ -test (A) or two-way ANOVA (C, E, G). \* $P < 0.05$ , \*\* $P < 0.01$ , \*\*\* $P < 0.001$ , \*\*\*\* $P < 0.0001$ , n.s = not significant.

Source data are available online for this figure.

STING. We further investigated these points of contact by examining the various MARCH5 truncation mutants. MARCH5 is a transmembrane protein present mainly in the outer mitochondrial membrane. It includes an N-terminal RING domain that functions as an E3 ubiquitin ligase and four C-terminal transmembrane domains (Sugiura *et al*, 2013). Given that STING and MARCH5 are located in different organelles, their interaction should occur in the cytosol. Thus, we prepared MARCH5 truncation mutants ( $\Delta$ Cyto1,  $\Delta$ Cyto2,  $\Delta$ Cyto3) lacking the regions exposed to the cytosol (Fig 3D). We found that STING showed a similar level of interaction with these MARCH5 truncation mutants as with WT MARCH5 (Fig 3D). Our quantitative PLA analysis of the interaction between STING and MARCH5 truncation mutants showed that WT and all the truncation mutant MARCH5 interact STING equivalently (Fig EV2B). This suggests a general cytosolic interaction between STING and MARCH5 that is robust to the loss of any individual cytosolic loop.

**MARCH5 mediates the K63-linked ubiquitination of STING**

We next asked whether the E3 ligase activity of MARCH5 is required for the activation of STING-mediated type I IFN production. First, we generated mSTING\_ *March5*<sup>-/-</sup> MEFs that stably express mouse STING. Then, we transfected them with a construct encoding human MARCH5 and stimulated the resulting cells with double-stranded interferon stimulatory DNA (dsISD) (Stetson & Medzhitov, 2006). We found that IFN- $\beta$  induction was restored in response to dsISD in mSTING\_ *March5*<sup>-/-</sup> MEFs expressing wild-type MARCH5 but not in the cells expressing a MARCH5 CS (C65/68S) mutant lacking its E3 ubiquitin ligase activity (Fig 4A). This indicates that the E3 ligase activity of MARCH5 is required for STING-mediated type I IFN induction.

Next, we asked whether MARCH5 mediates the ubiquitination of STING. We co-transfected HEK293T cells with constructs encoding HA-tagged full-length ubiquitin (HA-Ub), Flag-tagged mouse STING, and Myc-tagged wild-type (WT) or C65/68S mutant (CS) hMARCH5. Then, we performed an immunoprecipitation of STING using an anti-Flag antibody and quantified ubiquitination in the immunoprecipitate. Not only did transfection of Ub increase STING ubiquitination, MARCH5 increased it even further. However, the CS mutant MARCH5 did not exhibit the same increase as WT MARCH5 (Fig 4B), indicating that the catalytic activity of MARCH5 is necessary for STING ubiquitination. This function of MARCH5 is

conserved between mice and humans (Fig EV1B) as seen for STING-induced ISG56 production (Fig EV1A). To exclude the possibility that the ubiquitinated proteins were STING-associated proteins rather than STING itself, we co-transfected HEK293T cells with constructs encoding Myc-tagged mSTING with or without HA-tagged Ub, Flag-tagged hMARCH5, and then performed denaturation of cell lysates by SDS and boiling prior to immunoprecipitation. This treatment separates STING from any STING-associated proteins that could be ubiquitinated by MARCH5. After quenching the denaturing effects of SDS with excess lysis solution containing Triton X-100, we immunoprecipitated STING using an anti-Myc antibody and analyzed its ubiquitination status via immunoblotting. Under these denaturing conditions, we actually detected more ubiquitination associated with the addition of MARCH5, verifying a direct conjugation of STING to Ub (Fig 4C).

Based on previous reports that STING undergoes various ubiquitin-related modifications, we next asked which type of ubiquitin chain is conjugated to STING by MARCH5. We did this by quantifying STING ubiquitination in HEK293T cells co-transfected with plasmids encoding HA-tagged wild-type, K63-type or K48-type Ub, Myc-tagged human STING, and Flag-tagged human MARCH5. Although the addition of MARCH5 slightly increased K48-type ubiquitination of STING, there was a larger increase in K63-linked ubiquitination (Fig 4D). These results suggest MARCH5 predominantly confers K63-linked ubiquitination of STING.

Next, we sought to determine the residue of STING that is subject to MARCH5-mediated ubiquitination. We generated the mSTING KR mutants (K19R, K150/151R, K235R, K288R, K337R) by replacing the lysine residues that are conserved between human and mouse with arginine, and we then examined MARCH5-mediated STING ubiquitination in those mutants. For the K150/151R mutant mSTING, we mutated both the conserved K150 and its neighboring K151. Only the K19R mutant mSTING displayed decreased ubiquitination compared WT mSTING (Fig 4E), suggesting that the lysine 19 residue of mSTING could be ubiquitinated by MARCH5.

**ROS produced secondary to MARCH5 deficiency induces STING polymer formation**

Previous studies showed that STING activation leads to the formation of protein complexes that can be resolved as monomers, dimers, and higher molecular weight polymers. The higher

molecular weight STING polymers are known to be formed via intermolecular disulfide linkages (Ergun et al, 2019) and have been referred to as oligomers, polymers, and aggregates (Jin et al, 2010; Tanaka & Chen, 2012; Li et al, 2015; Haag et al, 2018; Ergun

et al, 2019; Zhang et al, 2019; Tao et al, 2020; Zamorano Cuervo et al, 2021). The majority of the STING oligomers have been regarded as an active form (Tanaka & Chen, 2012; Li et al, 2015; Ergun et al, 2019) but ROS-induced inactive STING polymers have

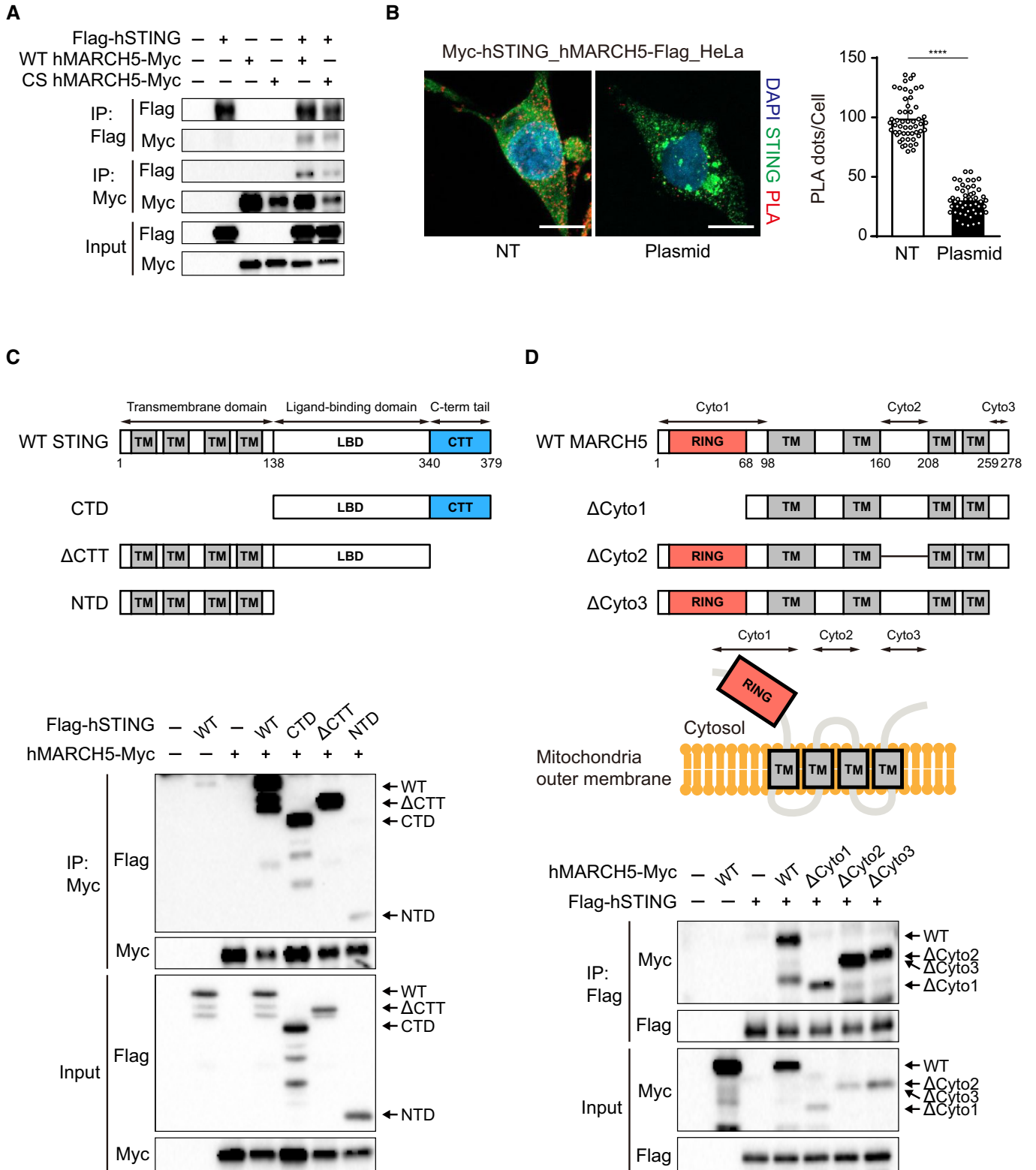


Figure 3.

**Figure 3. MARCH5 interacts with STING at steady state in the ER.**

- A** Flag-tagged hSTING (Flag-hSTING), Myc-tagged wild-type hMARCH5 (WT hMARCH5-Myc), and Myc-tagged hMARCH5 C65/68S mutant (CS hMARCH5-Myc) were expressed individually or together in HEK293T cells for 24 h. The cells were treated with MG132 (10  $\mu$ M) for 24 h to prevent MARCH5 degradation. Cell lysates were immunoprecipitated with anti-Flag or anti-Myc antibodies and then subjected to SDS-PAGE and immunoblotting with the indicated antibodies.
- B** HeLa cells stably expressing both Myc-tagged hSTING and Flag-tagged hMARCH5 were stimulated by transfection of plasmid DNA (5  $\mu$ g/ml) for 6 h. STING and STING-MARCH5 interactions were visualized by staining with an anti-Myc antibody (green) and in proximal ligation assays (PLA, red) using anti-Myc and anti-Flag antibodies. Confocal micrographs are shown on the left. Magnification, 630 $\times$ . Scale bars: 10  $\mu$ m. Quantification of the PLA dots ( $n = 50$ ) is shown in the right bar graph. Each dot represents the number of PLA dots within a cell (right). Data are presented as mean  $\pm$  SD.
- C, D** A schematic diagram of STING (C) and MARCH5 domains and topology (D). The numbers indicate hSTING and hMARCH5 amino acid residue positions. (C) Plasmids encoding Myc-tagged hMARCH5 and Flag-tagged hSTING full-length (FL) or truncation mutants (CTD: 138–379 amino acids,  $\Delta$ CTT: 1–339 amino acids, NTD: 1–138 amino acids) were co-transfected into HEK293T cells for 24 h, and the cells were treated with MG132 (10  $\mu$ M) for 24 h. Cell lysates were immunoprecipitated with an anti-Myc antibody and then subjected to SDS-PAGE and immunoblotting with the indicated antibodies. (D) Plasmids encoding Flag-tagged hSTING and Myc-tagged hMARCH5 FL or truncation mutants ( $\Delta$ Cyto1: 68–278 amino acids,  $\Delta$ Cyto2: 1–160 and 208–278 amino acids,  $\Delta$ Cyto3: 1–259 amino acids) were co-transfected into HEK293T cells for 24 h, and the cells were treated with MG132 (10  $\mu$ M) for 24 h. Cell lysates were immunoprecipitated with an anti-Flag antibody and then subjected to SDS-PAGE and immunoblotting with the indicated antibodies.

Data information: The data are representative of at least two independent experiments.  $n$ , number of samples (biological replicates). Statistical significance was analyzed by unpaired two-tail Student's  $t$ -test. \*\*\*\* $P < 0.0001$ .

Source data are available online for this figure.

been reported and called as STING aggregates (Zamorano Cuervo *et al.*, 2021). However, the activation status does not correlate with the structure of high molecular weight STING polymers. Several methods, including native PAGE (Tanaka & Chen, 2012; Haag *et al.*, 2018; Ergun *et al.*, 2019; Zhang *et al.*, 2019), non-reducing SDS-PAGE (Jin *et al.*, 2010; Tao *et al.*, 2020; Zamorano Cuervo *et al.*, 2021), and semi-denaturing detergent agarose gel electrophoresis (SDD-AGE) (Li *et al.*, 2015; Zamorano Cuervo *et al.*, 2021) have been used to analyze STING polymer structure, but none of these methods clearly determined the activity of each polymeric structure. To better understand how MARCH5 alters STING activity, we analyzed the conformation of STING stimulated by DMXAA via non-reducing SDS-PAGE with concentration titration (10, 25, 100  $\mu$ g/ml). Increasing concentrations of DMXAA induced the formation of STING polymers of high molecular weight. Interestingly, we observed more STING polymers in *March5*<sup>-/-</sup> MEFs than WT MEFs even without stimulation (Fig 5A). Since STING activity is impaired in *March5*<sup>-/-</sup> MEFs, we suspected that these high molecular weight STING molecules were inactive STING polymers. A follow-up SDD-AGE analysis confirmed increased formation of high molecular weight STING polymers in *March5*<sup>-/-</sup> MEFs compared to WT (Fig 5B). Notably, these STING polymers and high molecular weight forms of STING observed in non-reducing SDS-PAGE were reduced to monomeric forms in reducing gel, indicating that STING dimers and polymers are all formed through disulfide bonding (Fig 5B). Altogether, these data confirm MARCH5-deficient cell lines preferentially produce disulfide-bonded STING polymers.

We wanted to understand what induces STING polymer formation in *March5*<sup>-/-</sup> MEFs. Previous studies reported increased intracellular ROS in cell lines lacking MARCH5 (Park *et al.*, 2010; Nagashima *et al.*, 2019). Two recent studies found that increased intracellular ROS triggered STING oxidization, leading to inactive STING polymer formation (Tao *et al.*, 2020; Zamorano Cuervo *et al.*, 2021). Thus, we suspected that inactive STING polymers are formed because of elevated levels of intracellular ROS in *March5*<sup>-/-</sup> MEFs. Indeed, when we measured cellular ROS levels using 2',7'-dichlorodihydrofluorescein diacetate (DCFDA), we found that *March5*<sup>-/-</sup> MEFs produce significantly more ROS than WT MEFs (Fig 5C). These increased levels of intracellular ROS in *March5*<sup>-/-</sup> MEFs could be quenched, however, by treatment with the

antioxidant N-acetyl-cysteine (NAC). Next, we used the bio-switch method to examine protein oxidation by quantifying the conjugation of maleimide-(polyethylene glycol)<sub>2</sub>-biotin (maleimide-PEG<sub>2</sub>-biotin) to oxidized cysteine residues (Armstrong *et al.*, 2011; Zamorano Cuervo *et al.*, 2021). When we subjected whole cell lysates from WT and *March5*<sup>-/-</sup> MEFs to maleimide-PEG<sub>2</sub>-biotin labeling, we found increased protein oxidation in *March5*<sup>-/-</sup> MEFs compared to WT MEFs (Fig 5D). This is consistent with the higher ROS levels of *March5*<sup>-/-</sup> MEFs. Finally, we looked specifically at endogenous STING and found more STING oxidation in *March5*<sup>-/-</sup> MEFs than WT (Fig 5E). These results are consistent with a model in which *March5*<sup>-/-</sup> MEFs produce increased ROS levels, which then trigger STING oxidization and polymer formation.

To confirm that ROS trigger inactive STING polymer formation, we treated *March5*<sup>-/-</sup> MEFs with NAC to quench ROS and then quantified both STING polymer formation and ISG56 production upon DMXAA stimulation. Although NAC did reduce intracellular ROS levels in *March5*<sup>-/-</sup> MEFs, we did not see any reduction in STING polymers or increase in ISG56 production (Fig EV3A and B). We reasoned that existing ROS-triggered STING polymers might not unfold upon ROS quenching and that such polymers would interfere with the activity of newly synthesized STING. We therefore wanted to examine the effect of ROS quenching only on nascent STING molecules. Because STING is degraded after activation (Konno *et al.*, 2013), we first examined the timing of STING degradation and recovery. We found that STING was almost completely degraded after 8 h of treatment with DMXAA and only started to re-appear 18 h after DMXAA removal (Fig EV3C). We prevented oxidation of nascent STING molecules using NAC during this recovery period. Under these conditions, which should lead to degradation of any pre-existing STING, we found reduced STING polymers in NAC-treated *March5*<sup>-/-</sup> MEFs compared to untreated cells (Fig 5F). To better visualize these STING polymers, we treated cells with the cross-linking reagent DSP. We found that NAC-treated *March5*<sup>-/-</sup> MEFs showed less STING polymers and more monomers containing the active form (upper species) (Fig 5G). Finally, we found increased ISG56 production in NAC-treated *March5*<sup>-/-</sup> MEFs compared to untreated cells (Fig 5H). These results suggest that increased cellular ROS levels in *March5*<sup>-/-</sup> MEFs impair STING activity by promoting the formation of inactive STING polymers.



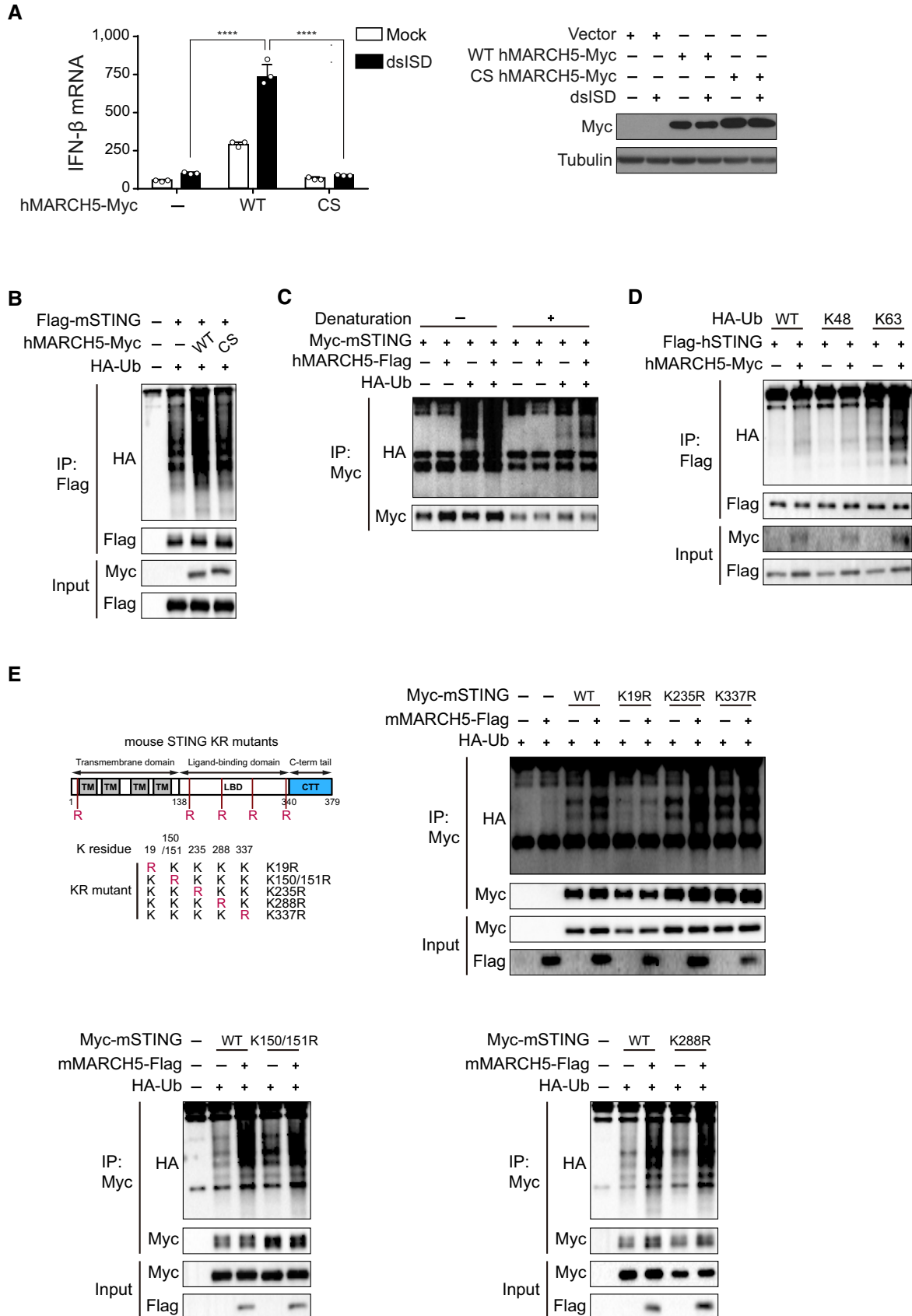


Figure 4.

**Figure 4. MARCH5 mediates K63-linked polyubiquitination of STING.**

- A *March5*<sup>-/-</sup> MEF cells stably expressing mouse STING were transfected with plasmids encoding Myc-tagged wild-type hMARCH5 (WT) or C65/68S mutant hMARCH5 (CS) for 24 h followed by transfection with dsISD (5 µg/ml) for 6 h. The induction of ISG56 mRNA was measured by RT-qPCR (left). Data are presented as mean ± SD (*n* = 3). MARCH5 expression was examined by SDS-PAGE followed by immunoblotting with an anti-Myc antibody. Tubulin, loading control (right).
- B HEK293T cells were co-transfected with plasmids encoding HA-tagged Ub (HA-Ub) together with those encoding Flag-tagged mSTING (Flag-mSTING) and Myc-tagged wild-type (WT) or C65/68S mutant (CS) hMARCH5 (hMARCH5-Myc) for 24 h. Cell lysates were immunoprecipitated with an anti-Flag antibody and then subjected to SDS-PAGE and immunoblotting with the indicated antibodies.
- C Plasmids encoding Myc-tagged mSTING (Myc-mSTING), Flag-tagged hMARCH5 (hMARCH5-Flag), and HA-tagged Ub (HA-Ub) were transfected individually or together into HEK293T cells for 36 h. Cell lysates were incubated in 1% SDS for denaturing at 95°C for 10 min. Native or denatured lysates were diluted in lysis buffer, immunoprecipitated with an anti-Myc antibody, and then subjected to SDS-PAGE and immunoblotting with the indicated antibodies.
- D HEK293T cells were transfected with plasmids encoding Flag-tagged hSTING (Flag-hSTING), Myc-tagged hMARCH5 (hMARCH5-Myc), and either HA-tagged wild-type Ub (WT) or mutant Ub (K48-only or K63-only linked Ub; K48 and K63, respectively) individually or together for 36 h. Cell lysates were immunoprecipitated with an anti-Flag antibody and subjected to SDS-PAGE and immunoblotting with the indicated antibodies.
- E A schematic diagram of mouse STING KR mutants. HEK293T cells were co-transfected with plasmids encoding HA-tagged Ub (HA-Ub) and Myc-tagged wild-type mSTING (WT) or mutant mSTINGs (K19R, K150/151R, K235R, K288R, K337R) with or without the one encoding Flag-tagged hMARCH5 (hMARCH5-Flag) for 36 h. Cell lysates were immunoprecipitated with an anti-Myc antibody and then subjected to SDS-PAGE and immunoblotting with the indicated antibodies.

Data information: The data are representative of at least two independent experiments. *n*, number of samples (biological replicates). Statistical significance was analyzed by two-way ANOVA. \*\*\*\**P* < 0.0001.

Source data are available online for this figure.

**MARCH5 suppresses oxidation-induced STING polymer formation**

Since we determined that STING polymer formation in *March5*<sup>-/-</sup> MEFs occurs via ROS-induced STING oxidation, we next asked whether ROS levels and polymer formation were altered in MARCH5 deficient cell lines with rescued MARCH5 expression. We found hMARCH5 *March5*<sup>-/-</sup> MEFs produce levels of cellular ROS similar to WT MEFs (Fig 6A). In addition, we found using non-reducing SDS-PAGE that hMARCH5 *March5*<sup>-/-</sup> MEFs do not exhibit STING polymer formation like *March5*<sup>-/-</sup> MEFs (Fig 6B). These data indicate that hMARCH5 expression rescues the high levels of cellular ROS that induce STING polymer formation in MARCH5-deficient cell lines.

Since stable expression of hMARCH5 reduces both ROS production and STING polymer formation, we next asked whether the catalytic activity of MARCH5 is required for both. After co-transfecting HEK293T cells with an hSTING-encoding plasmid and either a WT hMARCH5 or hMARCH5 CS (C65/68S) mutant-encoding plasmid, we examined STING polymer formation with or without ROS-inducing H<sub>2</sub>O<sub>2</sub> treatment. We found reduced STING polymer formation in the presence of WT hMARCH5, but not hMARCH5 CS mutant (Fig 6C). We did not, however, observe any change in ROS levels after transient transfection of hMARCH5 (Fig EV4A). Together, these results indicate that MARCH5 suppresses ROS-induced polymer formation and its subsequent inactivation of STING via its E3 ubiquitin ligase activity. Because we found that the lysine 19 residue of STING is subject to MARCH5-mediated ubiquitination (Fig 4E), we examined the ROS-induced polymer formation of the K19R mutant STING. Unlike wild-type STING, MARCH5 did not suppress the polymer formation of the K19R mutant STING (Fig 6D). These findings further support the notion that MARCH5 suppresses the formation of STING polymers by ubiquitinating STING.

Finally, we wanted to determine whether the detrimental effects of direct STING oxidation are counter-balanced by MARCH5-mediated ubiquitination. Reportedly, it is human STING cysteine 206 that is oxidized by ROS, leading to the formation of inactive STING aggregates (Zamorano Cuervo *et al*, 2021). The Cys205 residue of mSTING is equivalent of human STING Cys206. We therefore generated a mouse STING C205S mutant (mSTING\_C205S) in which Cys205 is replaced with serine. Consistent with the previous study, using a maleimide-PEG<sub>2</sub>-biotin labeling technique with transfected

HEK293T cells, we found reduced oxidation of mSTING\_C205S compared to WT mSTING (Fig 6E). Next, when we examined STING polymer formation upon H<sub>2</sub>O<sub>2</sub> treatment, we found significantly fewer polymers associated with mSTING\_C205S in oxidizing conditions compared to WT mSTING (Fig 6F). Finally, we asked whether a Cys205 to serine substitution in STING, which reduces STING oxidation and polymer formation itself, makes MARCH5 dispensable under oxidizing conditions for suppressing STING polymer and inactivation. We co-expressed WT mSTING or mSTING C205S mutant with or without WT hMARCH5 in HEK293T cells and then examined STING polymer formation. While WT mSTING polymer formation was inhibited by hMARCH5 but not by the CS (C65/68S) mutant hMARCH5 (Fig 6C), mSTING C205S polymer formation was unaffected by the presence of MARCH5 (Fig 6G). Of note, we found that MARCH5-mediated STING ubiquitination occurs similarly in WT STING, the C205S mutant mSTING and the S366A mutant hSTING which is not phosphorylated by TBK1 (Tanaka & Chen, 2012) (Fig EV5A and B). Together, these results indicate MARCH5-mediated ubiquitination of STING suppresses ROS-induced STING polymer formation and inactivation.

Based on the data presented in this study, we propose a model of how the E3 Ub ligase MARCH5 maintains STING activity in high ROS conditions in which STING is oxidized at cysteine (Cys 205 and 206 for mouse and human, respectively) and prone to form inactive polymers (Fig 6H). When MARCH5 is present, it mediates K63-linked poly-ubiquitination of STING, which prevents the formation of inactive STING polymers and preserves the activity of STING to induce type I-IFN production. But without MARCH5, MARCH5-mediated ubiquitination of STING is lost, and thus the formation of inactive STING polymers are enhanced, disrupting STING activation. In summary, our findings suggest MARCH5 serves as a guard protein to protect STING activity in high ROS environments by inhibiting oxidation-induced inactive STING polymer formation.

**Discussion**

While several PTMs reportedly regulate STING activity, when, where, and in which order these STING modifications occur and how they are integrated to determine overall STING activity remains

unclear. We previously identified an inter-organelle communication pathway in which STING signaling is regulated by mitochondrial dynamics and function. However, the molecular details underlying this ER-mitochondria communication has not been fully understood. Here, we provide evidence that points of contact between the

mitochondrial transmembrane E3 ubiquitin ligase MARCH5 and ER-localized STING contribute to the integrated control of STING activity. We demonstrate that increased production of cellular ROS in MARCH5-deficient cells increases STING oxidation, which then facilitates the formation of inactive STING polymers. We determined

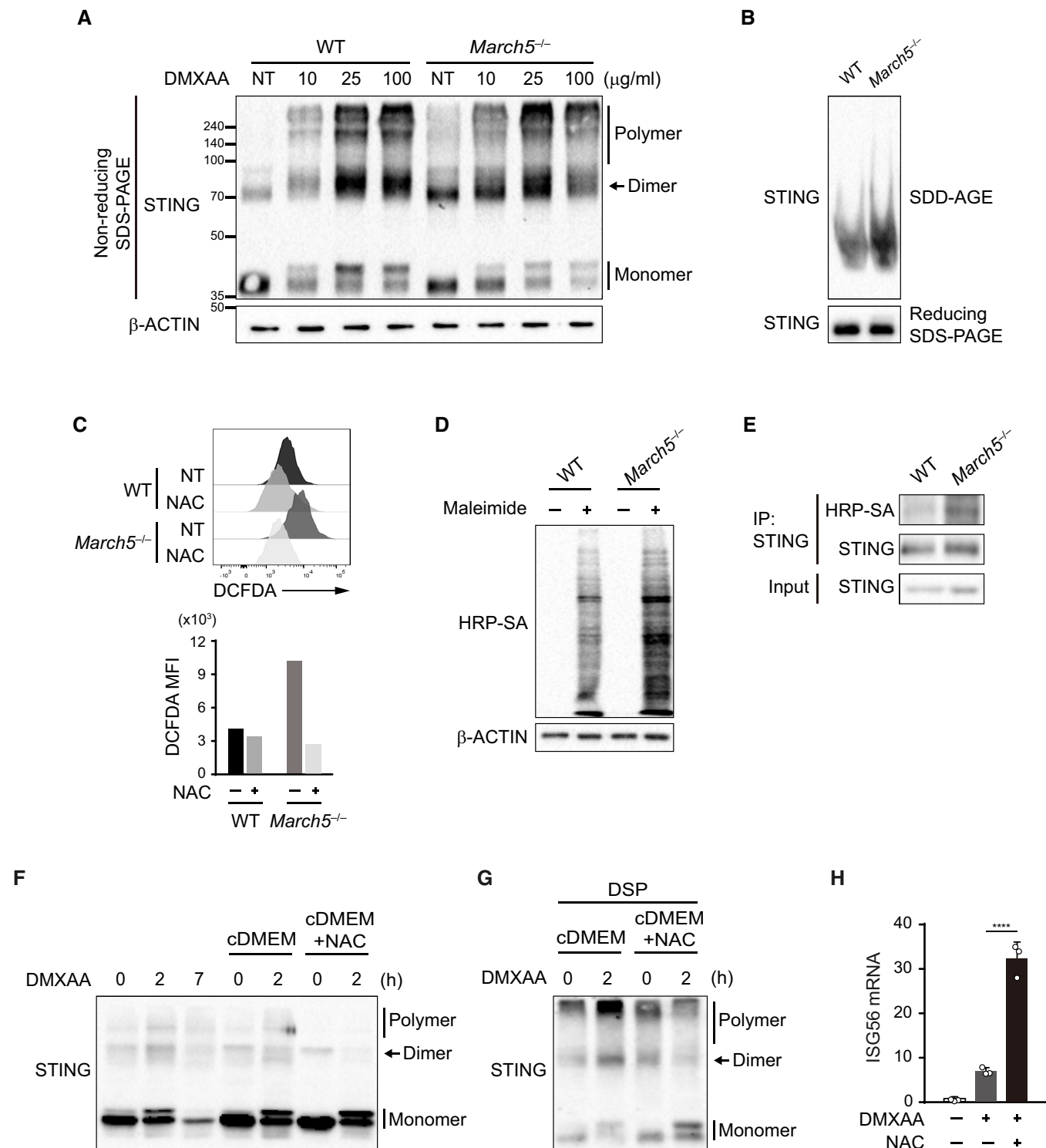


Figure 5.

**Figure 5. High level ROS in *March5*<sup>-/-</sup> MEF induces the STING polymer formation.**

- A Wild-type (WT) and *March5*<sup>-/-</sup> MEFs were stimulated with DMXAA (10, 25, 100 µg/ml) for 2 h. Cell lysates were resolved by non-reducing SDS-PAGE, and total STING and β-ACTIN were immunoblotted with the indicated antibodies.
- B Cell lysates of WT and *March5*<sup>-/-</sup> MEFs were resolved by SDD-AGE or reducing SDS-PAGE, and total STING was analyzed by immunoblotting with an anti-STING antibody.
- C WT and *March5*<sup>-/-</sup> MEFs were cultured with or without NAC (20 mM) for 12 h and then treated with DCFDA (5 µM) in Opti-MEM for 30 min. Flow cytometry analyses for measuring cellular ROS levels and their quantifications are shown in the upper histogram and lower bar graph, respectively. MFI, mean fluorescence intensity.
- D Cell lysates of WT and *March5*<sup>-/-</sup> MEFs were labeled with or without maleimide-PEG<sub>2</sub>-biotin and resolved by SDS-PAGE. Proteins conjugated with maleimide-PEG<sub>2</sub>-biotin were detected with horseradish peroxidase-conjugated streptavidin (HRP-SA). β-ACTIN, loading control.
- E Cell lysates of WT and *March5*<sup>-/-</sup> MEFs were denatured and immunoprecipitated with an anti-STING antibody and then labeled with maleimide-PEG<sub>2</sub>-biotin. The immunoprecipitates were resolved by SDS-PAGE, and maleimide-PEG<sub>2</sub>-biotin-conjugated STING was detected with HRP-SA. Immunoprecipitated STING was immunoblotted with an anti-STING antibody.
- F, G *March5*<sup>-/-</sup> MEFs were treated with DMXAA (100 µg/ml) for 2 or 7 h. After stimulation for 7 h, the culture medium was replaced with fresh cDMEM with or without NAC (20 mM), and the cells were cultured for another 16 h. Then, the cells were treated with DMXAA (100 µg/ml) alone or together with NAC (20 mM) for 2 h. (F and G) Cell lysates without (F) or with (G) pre-treatment with DSP (2 mM) on ice for 3 h were subjected to non-reducing SDS-PAGE and immunoblotting with an anti-STING antibody. The data are representative of two independent experiments.
- H *March5*<sup>-/-</sup> MEFs were treated with DMXAA (100 µg/ml) for 7 h. After stimulation for 7 h, the culture medium was replaced with fresh cDMEM with or without NAC (20 mM), and the cells were cultured for another 16 h. Then, the cells were treated with DMXAA (100 µg/ml) alone or together with NAC (20 mM) for 2 h. The induction of ISG56 mRNA was measured by RT-qPCR. Data are presented as mean ± SD (n = 3).

Data information: The data are representative of at least two independent experiments. n, number of samples (biological replicates). Statistical significance was analyzed by one-way ANOVA. \*\*\*\*P < 0.0001.

Source data are available online for this figure.

that STING polymer formation is suppressed by MARCH5 which catalyzes K63-linked ubiquitination on STING. Our results highlight the intricate regulation of STING activity by MARCH5, the activity of which balances STING ubiquitination and polymer formation.

Prior to our study, although STING activation and oxidative stress were known to induce higher order STING polymerization, the nature of these polymers was not clearly resolved biochemically, being instead inferred only from the effects different stimuli had on STING activity. In an initial report, STING agonists induced the formation of a smear of STING aggregates on native gels (Tanaka & Chen, 2012). Another group found that TBK1 supports the formation of phosphorylated STING aggregates (Li et al, 2015). More recently, cryo-EM studies revealed ligand-induced tetramerization of STING dimers (i.e., octamerization), which then form an active complex with TBK1. Upon ligand binding, the STING ligand binding domains (LBDs) close and undergo a 180° rotation, culminating in a side-by-side arrangement of four dimers (Shang et al, 2019; Zhang et al, 2019; Lu et al, 2022). Both the hyperactive STING mutations that cause STING-associated vasculopathy with onset in infancy (SAVI) and deletion of STING's autoinhibitory CTT domain led to the formation of higher order polymers that required interdimer disulfide bond formation (Ergun et al, 2019). It was unclear, however, whether the resulting high molecular weight STING polymers observed as smeared STING bands on gels are octameric polymers. Contrary to activation condition, an early study reported that H<sub>2</sub>O<sub>2</sub> treatment induced the formation high molecular weight form of oxidized STING that was analyzed on non-reducing SDS-PAGE, although the study focused on oxidized dimers rather than higher molecular weight polymers (Jin et al, 2010). Two recent studies showed that under conditions of oxidative stress, disulfide-containing inactive polymers (aggregates) are formed (Zamorano Cuervo et al, 2021) and active dimer formation is inhibited (Tao et al, 2020). Together, these studies seemed to suggest that STING forms active polymeric structures upon ligand stimulation and inactive polymer formation in the presence of even stronger agonistic or pathogenic stimulation. Under oxidative stress conditions, STING forms inactive polymers without the formation of intermediary

active polymer structures (Zamorano Cuervo et al, 2021). The structural differences between active and inactive polymers are not clearly delineated, but both forms seem to involve cysteine disulfide bond formation at Cys148 and Cys206 (amino acid numbers for hSTING). Further investigation will determine whether these cysteine residues form intra- or inter-dimer crosslinks.

Cellular redox signaling plays roles in regulating protein conformation, function, and homeostasis. Increased ROS levels induce protein aggregation, which is associated with aging and the proteinopathies of cataracts and neurodegenerative diseases like amyotrophic lateral sclerosis (ALS) (van Dam & Dansen, 2020). It has been shown that the protein aggregates are formed via cysteine oxidation that leads to the formation of either intramolecular or intermolecular disulfide bonds. The γD-crystallin mutants found in cataracts form intramolecular disulfide bonds (Serebryany et al, 2016), while the Cu, Zn-superoxide dismutase (SOD1) aggregates associated with familial ALS are characterized by intermolecular disulfide bonds (Deng et al, 2006; Furukawa et al, 2006; Toichi et al, 2013). The inclusions of trans-activation response (TAR) DNA-binding protein of 43 kDa (TDP-43) associated with ALS and frontotemporal lobar degeneration linked to TDP-43 pathology (FTLD-TDP) also contain intermolecular disulfide bonds (Cohen et al, 2012). Contrary to the harmful effects of high levels of ROS, lower levels of ROS seem to control diverse intracellular phenomena, including inflammatory signaling pathways. Such redox-dependent signaling occurs via the reversible oxidation of signaling molecule cysteines (Holmström & Finkel, 2014). Both the RLR and the inflammasome signaling have been shown to require mitochondrial ROS (Tal et al, 2009; Zhou et al, 2010, 2011), but the mechanisms by which ROS regulate them are not fully understood. It is also unclear whether any of the related signaling molecules are modified via ROS-dependent cysteine oxidation. One early study found that activated MAVS forms prion-like aggregates (Hou et al, 2011) that are functionally active and that seem to propagate RIG-I signaling in mitochondria. Interestingly, these MAVS aggregates are disaggregated via treatment with the reducing agent DTT, implying that they contain disulfide bonds. Similarly, activated

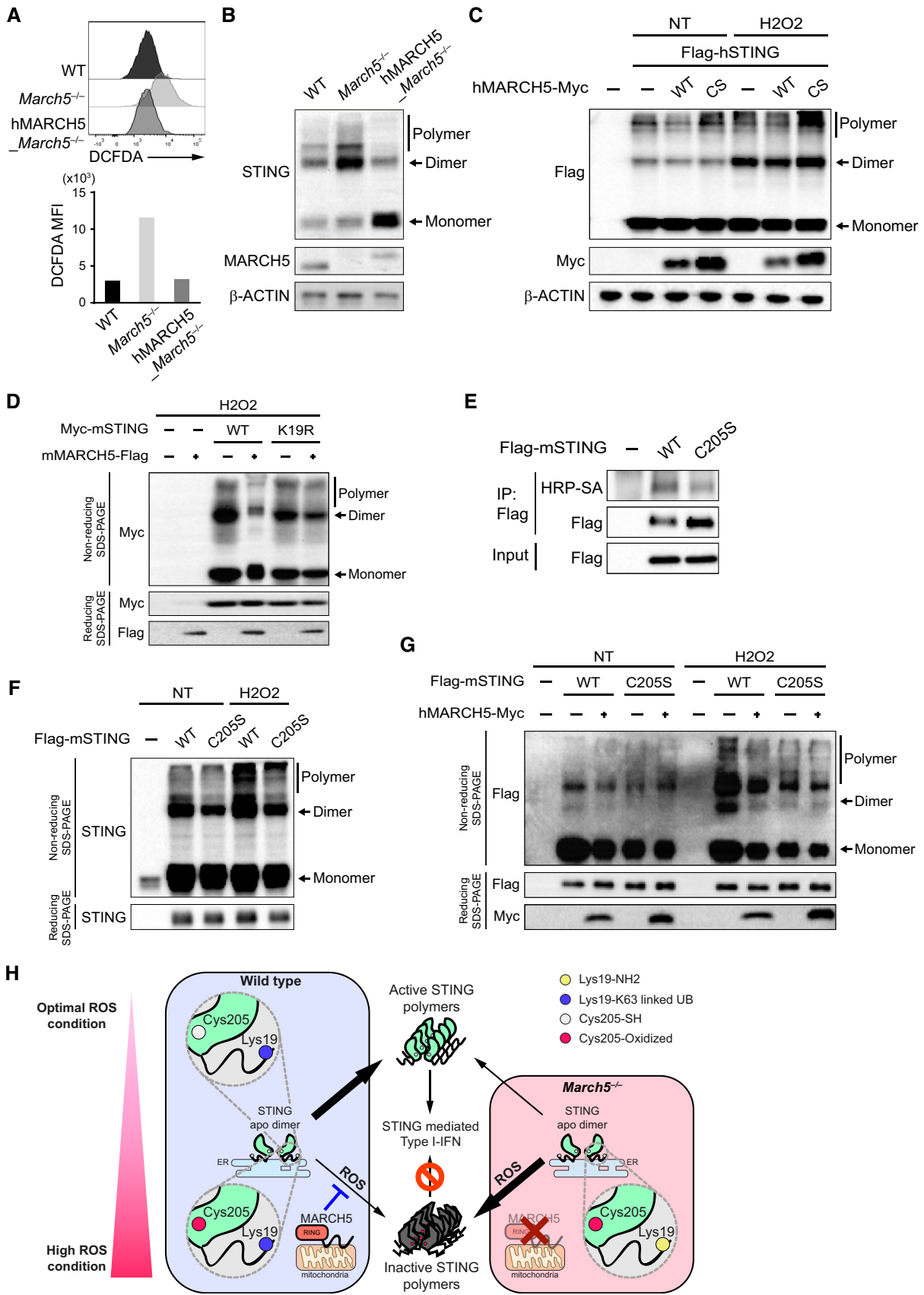


Figure 6.

**Figure 6. MARCH5 blocks oxidation-induced STING polymer formation.**

- A WT MEFs, *March5*<sup>-/-</sup> MEFs, and *March5*<sup>-/-</sup> MEFs stably expressing hMARCH5 (*hMARCH5\_March5*<sup>-/-</sup>) were treated with DCFDA in Opti-MEM (5  $\mu$ M) for 30 min. Flow cytometry analyses for measuring cellular ROS levels and their quantifications are shown in the upper histogram and lower bar graph, respectively. MFI, mean fluorescence intensity.
- B Cell lysates of WT, *March5*<sup>-/-</sup>, and *hMARCH5\_March5*<sup>-/-</sup> MEFs were resolved by non-reducing SDS-PAGE. STING, MARCH5, and  $\beta$ -ACTIN were detected by immunoblotting with the indicated antibodies.
- C Plasmids encoding Flag-tagged hSTING (Flag-hSTING), Myc-tagged wild-type hMARCH5 (WT), and Myc-tagged C65/68S mutant hMARCH5 (CS) were transfected individually or together in HEK293T cells for 24 h. The cells were then treated with or without H<sub>2</sub>O<sub>2</sub> (5 mM) in DPBS for 30 min. Cell lysates were resolved by non-reducing SDS-PAGE, and then STING, MARCH5 and  $\beta$ -ACTIN were detected by immunoblotting with the indicated antibodies.
- D HEK293T cells were co-transfected with plasmids encoding Myc-tagged WT or K19R mutant mSTING with or without the one encoding Flag-tagged mMARCH5 (mMARCH5-Flag) for 24 h and then treated with H<sub>2</sub>O<sub>2</sub> (5 mM) for 30 min. Cell lysates were resolved by reducing or non-reducing SDS-PAGE, and STING and MARCH5 were detected by immunoblotting with the indicated antibodies.
- E Flag-tagged WT or C205S mutant mSTING-encoding plasmids were transfected into HEK293T cells for 24 h. Cell lysates were denatured and immunoprecipitated with an anti-Flag antibody. Maleimide-PEG<sub>2</sub>-biotin-conjugated STING was detected as in Fig 5E.
- F HEK293T cells were co-transfected with plasmids encoding Myc-tagged WT or C205S mutant mSTING for 24 h and then treated without (NT) or with H<sub>2</sub>O<sub>2</sub> (5 mM) for 30 min. Cell lysates were resolved by reducing or non-reducing SDS-PAGE, and then STING was detected by immunoblotting with an anti-STING antibody.
- G Flag-tagged WT or C205S mutant mSTING-encoding plasmids with or without Myc-tagged wild-type hMARCH5 (*hMARCH5-Myc*) were co-transfected into HEK293T cells for 24 h. Then, the cells were treated with or without H<sub>2</sub>O<sub>2</sub> (5 mM) for 30 min. Cell lysates were resolved by reducing or non-reducing SDS-PAGE, and then total STING was analyzed via immunoblotting with the indicated antibodies.
- H Schematic depicting the regulation of the formation of higher order STING polymers by MARCH5-mediated K63-linked STING ubiquitination at lysine 19. STING ubiquitination prevents the formation of inactive STING polymers that can occur when cysteine 205 is oxidized in the presence of high levels of ROS.

Data information: The data are representative of at least two independent experiments.

Source data are available online for this figure.

STING forms DTT-sensitive polymers. Thus, based on the models proposed in previous studies (Ergun *et al.*, 2019; Zamorano Cuervo *et al.*, 2021), both MAVS and STING seem to initially form reversible polymers with disulfide bonds formed through redox signaling that only later become irreversible and inactive terminal aggregates. These terminal aggregates, which also seem to form in conditions of high oxidative stress, may be subject to clearance via autophagy. This time-dependent regulation of STING activity by ROS may reconcile the discordant reports on redox-dependent STING regulation (Jin *et al.*, 2010; Olganier *et al.*, 2018; Gunderstofte *et al.*, 2019; Tao *et al.*, 2020; Zamorano Cuervo *et al.*, 2021).

Like STING, it was shown that RLR signaling is also regulated by MARCH5. MARCH5 suppresses excessive and harmful RLR-mediated immune responses by conferring K48-linked ubiquitination on RIG-I and MAVS aggregates and targeting them for degradation (Yoo *et al.*, 2015; Park *et al.*, 2020). Although MARCH5 functions to reduce protein aggregates in both the RLR and STING pathways, there are clear differences in its function in each pathway. First, in contrast to its role with RLR, MARCH5 catalyzes the addition of K63-linked polyubiquitin chains to STING, which prevents its polymer rather than inducing its degradation. We did not observe any increase of active form of STING in the absence of MARCH5. Instead, we frequently observed the increase of STING when MARCH5 was co-expressed (Fig 4C and D). Thus, it is possible that MARCH5 stabilizes STING, which requires further investigation. Second, MARCH5's interaction with MAVS is induced by and therefore occurs after RIG-I stimulation (Yoo *et al.*, 2015). MARCH5's interaction with STING, however, occurs prior to stimulation and leads to its dissociation from activated STING (Fig 3B). This suggests that MARCH5 increases the threshold for oxidation-induced STING polymer formation. One recent study showed that another mitochondrial outer membrane protein, mitochondrial E3 ubiquitin protein ligase 1 (MUL1, aka MAPL), plays a similar role to MARCH5 in STING activation via K63-linked ubiquitination (Ni *et al.*, 2017). Further investigation will be required to determine whether MUL1 and MARCH5 work redundantly or function in distinct contexts.

Here, we focused on the regulation of STING activity by MARCH5 under high ROS environment (*March5*<sup>-/-</sup> MEFs or addition of H<sub>2</sub>O<sub>2</sub>). However, it is currently unclear whether MARCH5 regulates STING activation in normal ROS condition in the same way as it does in high ROS condition. Consistent with our results, stable MARCH5 knockdown and knockout cell lines exhibit increased ROS levels (Park *et al.*, 2010; Nagashima *et al.*, 2019). We observed, however, that transient, siRNA-mediated MARCH5 knockdown did not increase ROS levels or inhibit STING signaling (Fig EV4B and C). The oxidized STING and high molecular weight STING polymers were barely detected in WT MEFs in contrast to *March5*<sup>-/-</sup> MEFs at steady state. However, our gain-of-function approach demonstrated that transient expression of MARCH5 enhances STING activation in HEK293T, HaCaT cells, and WT MEFs (Fig 1A–E). Furthermore, we were able to detect high molecular weight STING polymers when STING was expressed by transfection (Fig 6C, F and G). The polymer formation of transiently expressed STING was suppressed by MARCH5 (Fig 6C) and substitution of Cys205 to serine even without H<sub>2</sub>O<sub>2</sub> supplement (Fig 6F and G). When we examined the ROS level in transfected cells, we found that plasmid transfection alone could cause some level of ROS induction (Fig EV4D). Therefore, although we cannot completely exclude a role for MARCH5 in regulating STING at low/normal ROS levels, MARCH5's regulation of STING seems contingent on oxidative conditions.

Here, we propose that MARCH5-mediated ubiquitination sets the threshold for oxidation-mediated STING polymer formation (Fig 6H). There are several remaining questions, however, that will have to be answered by future investigations. Although we showed that MARCH5 deficiency leads to STING signaling inhibition associated with an increase in inactive STING polymer formation, there is still work to be done on delineating the exact mode of action and its sequence. We frequently observed slight increases in STING phosphorylation in *March5*<sup>-/-</sup> MEFs compared to WT MEFs prior to ligand stimulation (Fig 2D and F). Currently, we cannot exclude the possibility that MARCH5 deficiency facilitates a reversible intermediary polymerization of STING that only later reaches an inactive

polymer state that shuts down STING signaling. Moreover, previous studies and our results showed that high molecular weight STING polymers are only a fraction of the STING molecules resolvable via non-reducing SDS-PAGE. This raises the question of how such a minor population suppresses STING signaling overall. It is possible that the high molecular weight polymers act via a dominant negative mechanism. Or the high molecular weight polymers are actually a mixture of STING monomers, dimers, and polymers that interact weakly with one another and that are disrupted upon SDS-PAGE. Last, the polymers may exist transiently on their way to terminal aggregation. In this scenario, SDS-PAGE-based analyses would provide snapshots that capture only the species that exist at the time of the analysis. Distinguishing among these possibilities will require a more sophisticated time-lapse and structural analysis.

Cryo-EM studies showed that TBK1-mediated STING phosphorylation requires the formation of a rather tightly packed array of STING dimers (octamer) (Ergun et al, 2019; Shang et al, 2019; Zhang et al, 2019), although a recent study suggests that such side-by-side packing and ER intermembrane head-to-head packing render STING in an inactive polymer conformation (Liu et al, 2023). However, the exact structures adopted by STING multimers decorated with various PTMs, including ubiquitination, are unknown. A single Ub molecule spans roughly 20 Å (PDB 3HM3). We demonstrated that the lysine 19 residue of STING is the target of MARCH5-mediated ubiquitination and suppression of STING polymer formation (Figs 4E and 6D). When we estimated the distance between the lysine residue and the closest amino acid residues in the neighboring STING dimer of a STING octamer (PDB 7SII), the gap was shorter than the diameter of a single Ub molecule. Considering the bulkiness of poly-Ub chains and depending on positioning, the octameric STING polymer array may be disrupted or distorted by Ub-conjugation. This could then decrease the chance with which cysteine residues on adjacent molecules form intermolecular disulfide bonds that lead to polymer formation. We showed that substitution of mSTING Cys205 to serine reduced oxidation-induced polymer formation regardless of the presence of MARCH5. The similarity between the structures of human and mouse STING allows us to infer that mSTING Cys205 is situated near the tetramer interface of two neighboring STING dimers. Thus, we speculate that MARCH5-mediated ubiquitination of STING at Lys19 may disrupt the interaction between the STING dimers. This steric hindrance may suppress the process of STING polymer formation mediated by Cys205 oxidation. This speculation should be validated via a structural analysis of poly-ubiquitinated STING polymers.

In summary, we found a novel mechanism regulating STING signaling in which MARCH5-mediated ubiquitination prevents oxidation-induced inactive STING polymer formation. We expect our results will further clarify the mechanisms underlying the various autoimmune, autoinflammatory, and neurological diseases to which STING contributes and provide new therapeutic strategies for targeting STING polymer formation.

## Materials and Methods

### Reagents

Chemical reagents were purchased as follows: 5,6-dimethylxanthone-4-acetic acid (DMXAA) (Sigma-Aldrich, USA); 2'-3' cyclic

GMP-AMP (cGAMP) (Biolog, Germany); double-stranded interferon stimulatory DNA (dsISD) (Invitrogen, USA); dimeric amidobenzimidazole (diABZI) (Invivogen, USA); Dithiobis(succinimidyl propionate) (DSP) (ProteoChem, USA); MG132 (Calbiochem, USA); N-Acetyl-L-cysteine (NAC) (Sigma-Aldrich, USA). Plasmid DNA, cGAMP, and dsISD were transfected using Lipofectamine 3000 (Invitrogen, USA) according to the manufacturer's instructions. As a mock control, only Lipofectamine 3000 was added. The following list indicates the antibodies used in this study and their provenance. Rabbit anti-TBK1 (Cat# 3504), rabbit anti-p-TBK1 (Cat# 5483), rabbit anti-IRF3 (Cat# 4302), rabbit anti-p-IRF3 (Cat# 4947), rabbit anti-STING (Cat# 13647), rabbit anti-p-STING (Cat# 72971), rabbit anti-p-STING (Cat# 19781), rabbit anti-Flag (Cat# 14793), and rabbit anti-β-ACTIN (Cat# 4970) were purchased from Cell Signaling (USA). Rabbit anti-Myc (Cat# ab9106) and rabbit anti-GM130 (Cat# ab52649) were purchased from Abcam (UK). Mouse anti-Flag (Cat# F1804) and mouse anti-Tubulin (Cat# T9026) were purchased from Sigma-Aldrich (USA). Rabbit anti-MARCH5 (Cat# LS-C164034) were purchased from LSBio (USA).

### Cell lines

Mouse embryonic fibroblast (MEF) cells, HeLa cells, HaCaT cells, and HEK293T cells were cultured in Dulbecco's modified Eagle's medium (DMEM) (Welgene, South Korea) supplemented with 10% heat-inactivated fetal bovine serum (Gibco, USA), 2 mM L-glutamine (Gibco, USA), 10 mM HEPES (Hyclone, USA), and 100 unit/ml penicillin/streptomycin (Gibco, USA) in a 5% CO<sub>2</sub> incubator at 37°C. MARCH5-floxed MEFs and control WT MEFs containing Cre-ERT2 were kindly provided by Dr. Shigeru Yanagi (Tokyo University, Japan) (Sugiura et al, 2013). We established *March5*<sup>-/-</sup> MEFs by treating MARCH5-floxed MEFs with tamoxifen for 1 month to flox out MARCH5. We confirmed a loss of MARCH5 expression by RT-PCR and immunoblotting. Retroviral vectors encoding human MARCH5 (hMARCH5) were generated via the method that follows. Briefly, hMARCH5 was amplified from hMARCH5-Myc\_pcdNA3.1(+) via polymerase chain reaction using the following primers: (forward) 5'-ATCTCGAGCTCAAGCTTACCATGCCGGACCAAGC-3'; (reverse) 5'-TCCAAAATTCGAAGCTTTTGCTTCTTCTGTCT-3'. The resulting PCR products were subcloned into the pLPCX retroviral vector. We generated HeLa cells and *March5*<sup>-/-</sup> MEFs that stably express human MARCH5 via the following method. HeLa cells expressing Myc-human STING were previously described (Kwon et al, 2017a). These cells and *March5*<sup>-/-</sup> MEFs were transduced with a retroviral vector expressing MARCH5 and treated with puromycin (2 μg/ml) to establish cell lines stably expressing hMARCH5. We generated WT or *March5*<sup>-/-</sup> MEFs stably expressing Myc-tagged mouse STING. WT and *March5*<sup>-/-</sup> MEFs were transduced with a retroviral vector expressing Myc-mouse STING and then treated with puromycin (2 μg/ml) to establish stable mSTING-expressing cell lines.

### Small interfering RNA experiments

MEF cells were reverse transfected with small interfering RNAs (siRNA; 50 nM) for 48 h using RNAiMAX (Invitrogen, USA) according to the manufacturer's instructions. The siRNAs used in these experiments were as follows: si*March5* #1 (Horizon, Cat# L-

057048-01); si*March5* #2: 5'-GGUUUAUGUCUUGGAUCUUGUU-3'; siCtrl: 5'-CCUACGCCACCAAUUUCGU-3'.

### Quantitative real-time PCR

Total RNA was isolated from cultured cells using the TRI reagent (Thermo Fisher Scientific, USA) according to the manufacturer's instructions. RNA concentrations were measured using a NanoDrop (Thermo Fisher Scientific, USA), and equal amounts of RNA for each sample were treated with DNase I (Promega, USA) to remove residual DNA. Complementary DNA (cDNA) was synthesized using oligo dT and SuperiorScript III (Enzynomics, South Korea) according to the manufacturer's instructions. Quantitative real-time PCR was performed with target gene primer sets using qPCR 2× Pre-MIX (SYBR Green with low ROX) (Enzynomics, South Korea) in a Rotor-Gene Q PCR machine (Qiagen, Germany). The sequences of the primers used were as follows: *Isg56* sense: 5'-CTCTGAAAGTG GAGCCAGAAAAC-3'; *Isg56* antisense: 5'-AAATCTTGCGGATAGGC TACGA-3'; *Ifn-β* sense: 5'-ATGGTGGTCCGAGCAGAGAT-3'; *Ifn-β* antisense: 5'-CCACCACTCATTCTGAGGCA-3'; *March5* sense: 5'-CCTCTGTTAACAGGAGGAAG-3'; *March5* antisense: 5'-GGAAACT GACCCTTCACATC-3'; *β-Actin* sense: 5'-ACCAACTGGGACGACAT GGAGAA-3'; *β-Actin* antisense: 5'-AGCCAGGTCCAGACGCAGGAT GG-3'. Transcript amounts were measured as cycle threshold (CT) values, and the data were analyzed via the  $\Delta\Delta CT$  method. Target gene mRNA expression was normalized to *β-Actin* expression.

### IFN-β promoter reporter luciferase assay

WT or *March5*<sup>-/-</sup> MEFs cells seeded on 24-well plates were transfected with plasmids pGL3-IFN-β luciferase (0.35 μg), pIRES-neo-β-gal (0.2 μg) as control, and indicated gene plasmid (0.45 μg). The cells were then lysed 24 h after the transfection with reporter lysis buffer (Promega, USA). After incubating the lysates with luciferase assay buffer (Promega, USA) and β-gal assay buffer (Promega, USA) at 37°C, their luminescence was measured with the GloMax®-Multi Detection System (Promega, USA).

### Immunofluorescence

Cells were grown on coverslips, fixed in 3.7% formaldehyde in PBS buffer, and then permeabilized with 0.1% saponin (Sigma-Aldrich, USA) in PBS buffer containing 5% bovine calf serum (BCS), 10 mM glycine, and 10 mM HEPES (pH 7.4). The cells were incubated with primary antibodies followed by Alexa Fluor™ 488-conjugated goat anti-mouse IgG or Alexa Fluor™ 594-conjugated goat anti-rabbit IgG antibodies (Thermo Fisher Scientific, USA). Micrographs were captured with a Zeiss LSM780 confocal microscope using the ZEN software (Carl Zeiss, Germany).

### Proximity ligation assay (PLA)

Proximity ligation assays were performed using the Duolink® *In Situ* Red Starter kit (Sigma-Aldrich, USA). HeLa cells stably expressing Myc-tagged human STING and Flag-tagged human MARCH5 were grown on coverslips, stimulated with plasmids (5 μg/ml) for 6 h, fixed in 3.7% formaldehyde in PBS buffer, permeabilized with 0.1% saponin (Sigma-Aldrich, USA) in PBS buffer containing 5%

bovine calf serum (BCS), 10 mM glycine, and 10 mM HEPES (pH 7.4), and then blocked with Duolink® Blocking solution. The cells were incubated with primary antibodies (anti-Flag mouse Ab and anti-Myc rabbit Ab) in Duolink® Antibody Diluent for 30 min. Next, the cells were incubated with Duolink® PLA probes, PLA anti-mouse MINUS, and PLA anti-rabbit PLUS in Duolink® Antibody Diluent for 1 h at 37°C before being washed with wash buffer A. Thereafter, the ligation solution was added to the cells and incubated for 30 min at 37°C, followed by washing with wash buffer A. For amplification, the cells were incubated with amplification solution for 110 min at 37°C and then washed with wash buffer B. Then, STING was counterstained by incubating the cells with Alexa Fluor™ 488-conjugated goat anti-rabbit IgG (Thermo Fisher Scientific, USA) for 20 min in the dark. After a final wash with 0.01× wash buffer B, the cells were mounted with Duolink® PLA Mounting Medium, and the nuclei were stained. Samples were examined with a Zeiss LSM880 confocal microscope using the ZEN software (Carl Zeiss, Germany).

### Immunoblot analysis and immunoprecipitation assay

Cells were lysed in 100 μl of lysis buffer containing 1% Triton X-100, 5 mM iodoacetamide (IAA), 0.5 mM phenylmethylsulfonyl fluoride (PMSF), 1 mM Na<sub>3</sub>VO<sub>4</sub>, and 1 mM NaF in PBS (10 mM Na<sub>2</sub>HPO<sub>4</sub>, 1.8 mM KH<sub>2</sub>PO<sub>4</sub>, 137 mM NaCl, 2.7 mM KCl, pH 7.4) at 4°C for 1 h. For the DSP cross-link condition, the cells were lysed in lysis buffer with DSP (2 mM) at 4°C for 3 h. The lysates were quenched with 100 mM Tris buffer at 4°C for 15 min and then centrifuged at 16,100 g at 4°C for 10 min. The protein concentrations of the supernatants were measured with a bovine serum albumin (BSA) assay kit (Invitrogen, USA). The samples were subjected to denaturation by boiling at 95°C for 10 min in sample buffer containing 1% SDS, 10% glycerol, 0.05% bromophenol blue (BPB) in 6.25 mM Tris buffer (pH 6.8) with (reducing) or without (non-reducing) 5% β-mercaptoethanol. For immunoprecipitation, the cell lysates were incubated with antibodies and protein G Sepharose® beads (GE Healthcare, USA) at 4°C for 3 h. They were then denatured by boiling at 95°C for 10 min in non-reducing SDS sample buffer. For the denaturation condition, the cell lysates were boiled at 95°C for 10 min in 1% SDS before adding the protein G Sepharose® beads. Then, lysis buffer was added to dilute the SDS to 0.1% before immunoprecipitation. The proteins were separated by 10% SDS-PAGE, blotted to a polyvinylidene difluoride (PVDF) membrane (Merck Millipore, USA), detected with primary antibodies and horseradish peroxidase (HRP)-conjugated secondary antibodies (Jackson Laboratory, USA), and visualized with the Luminata Crescendo Western HRP substrate (Merck Millipore, USA).

### Semi-denaturing detergent agarose gel electrophoresis (SDD-AGE)

Cells were lysed in lysis buffer containing 1% Triton X-100, 5 mM IAA, 0.5 mM PMSF, 1 mM Na<sub>3</sub>VO<sub>4</sub>, and 1 mM NaF in TBS (10 mM Tris, 150 mM NaCl, pH 7.4), and then centrifuged at 16,100 g at 4°C for 10 min. After measuring the protein concentrations of the supernatants with a BSA assay kit, the samples were mixed with 4× loading dye containing 20% glycerol, 8% SDS, and 0.2% bromophenol blue (BPB) in 2× tris-acetate-EDTA (TAE) buffer at RT for 10 min.



The proteins were separated on a 1.5% agarose gel in running buffer containing 0.1% SDS in 1× TAE at 4°C, blotted to a PVDF membrane, detected with primary antibodies and HRP-conjugated secondary antibodies, and visualized with the Luminata Crescendo Western HRP substrate.

### ROS measurements

Cells were washed once with Dulbecco's PBS (DPBS) and then incubated with 2',7'-dichlorodihydrofluorescein diacetate (DCFDA) (Invitrogen, USA) (5 μM) in Opti-MEM solution for 30 min in a 5% CO<sub>2</sub> incubator at 37°C. After washing the cells with DPBS, the DCFDA-positive cells were detected by flow cytometry (LSRFor-tessa) (BD Biosciences, USA). The data were analyzed and visualized with the FlowJo software package (BD Biosciences, USA).

### STING PTM-Oxy

Cells were lysed in lysis buffer containing 1% Triton X-100, 0.5 mM PMSF, 1 mM Na<sub>3</sub>VO<sub>4</sub>, and 1 mM NaF in PBS, and then centrifuged at 16,100 g at 4°C for 10 min. The supernatants were subject to denaturation by boiling at 95°C for 10 min in 1% SDS lysis buffer and then incubated in N-ethylmaleimide (NEM) (5 mM) at room temperature (RT) for 30 min. Samples were immunoprecipitated with anti-STING or anti-Myc antibodies plus Protein G Sepharose® beads (GE Healthcare, USA) at 4°C overnight. The immunoprecipitates were washed three times with 0.1% Triton X-100 in PBS and then incubated with 5 mM Tris (2-carboxyethyl) phosphine hydrochloride (TCEP) in lysis buffer (Merck Millipore, USA) at RT for 1 h. This was followed by an incubation with 1 mM maleimide-PEG<sub>2</sub>-biotin (Thermo Fisher Scientific, USA) in lysis buffer at RT for 2 h. The samples were then boiled at 95°C for 10 min in reducing SDS sample buffer, separated via 10% SDS-PAGE, and blotted to a PVDF membrane. Maleimide-PEG<sub>2</sub>-biotin-labeled proteins were detected with HRP-conjugated streptavidin (Invitrogen, USA) and visualized with the Luminata Crescendo Western HRP substrate.

### Statistical analysis

Data were analyzed using the GraphPad PRISM 6 software. Unpaired two-tail Student's *t*-test or ANOVA was performed. The results are expressed as means ± SD or SEM (represented as error bars). Significance was indicated with *P*-values: \**P* < 0.05, \*\**P* < 0.01, \*\*\**P* < 0.001, \*\*\*\**P* < 0.0001.

## Data availability

This study includes no data deposited in external repositories.

**Expanded View** for this article is available [online](#).

### Acknowledgements

We thank our colleagues in the lab for helpful discussions. We are also grateful to Dr. S. Ishido (Hyogo College of Medicine) and Dr. S. Yanagi (Tokyo University of Pharmacy and Life Science) for providing cell lines (MARCH5-floxed MEFs), to Dr. K.C. Chin (A\*STAR) for pGL3-IFN-β luciferase, and to Dr. M.J. Song (Korea University) for pIRES-neo-β-gal. This work was supported by

the National Research Foundation of Korea (NRF) grant funded by the Korea government (Ministry of Science and ICT) (NRF-2019R1A2C2085729).

### Author contributions

**Eunchong Eom:** Data curation; formal analysis; validation; investigation; visualization; methodology; writing – original draft; writing – review and editing. **Dohyeong Kwon:** Conceptualization; data curation; formal analysis. **Kyungpyo Son:** Conceptualization; data curation; formal analysis; validation; investigation; visualization; methodology; writing – original draft; project administration; writing – review and editing. **Suk-Jo Kang:** Conceptualization; data curation; formal analysis; supervision; funding acquisition; validation; investigation; methodology; writing – original draft; project administration; writing – review and editing. **Seokhwan Jeong:** Data curation; formal analysis; validation; investigation; visualization; methodology; writing – original draft; writing – review and editing.

### Disclosure and competing interests statement

The authors declare that they have no conflict of interest.

## References

- Ablasser A, Goldeck M, Cavlar T, Deimling T, Witte G, Rohl I, Hopfner KP, Ludwig J, Hornung V (2013) cGAS produces a 2'-5'-linked cyclic dinucleotide second messenger that activates STING. *Nature* 498: 380–384
- Armstrong AE, Zerbes R, Fournier PA, Arthur PG (2011) A fluorescent dual labeling technique for the quantitative measurement of reduced and oxidized protein thiols in tissue samples. *Free Radic Biol Med* 50: 510–517
- Barber GN (2014) STING-dependent cytosolic DNA sensing pathways. *Trends Immunol* 35: 88–93
- Bauer J, Bakke O, Morth JP (2017) Overview of the membrane-associated RING-CH (MARCH) E3 ligase family. *N Biotechnol* 38: 7–15
- Cohen TJ, Hwang AW, Unger T, Trojanowski JQ, Lee VM (2012) Redox signalling directly regulates TDP-43 via cysteine oxidation and disulphide cross-linking. *EMBO J* 31: 1241–1252
- Decout A, Katz JD, Venkatraman S, Ablasser A (2021) The cGAS–STING pathway as a therapeutic target in inflammatory diseases. *Nat Rev Immunol* 21: 548–569
- Deng H-X, Shi Y, Furukawa Y, Zhai H, Fu R, Liu E, Gorrie GH, Khan MS, Hung W-Y, Bigio EH (2006) Conversion to the amyotrophic lateral sclerosis phenotype is associated with intermolecular linked insoluble aggregates of SOD1 in mitochondria. *Proc Natl Acad Sci USA* 103: 7142–7147
- Dobbs N, Burnaevskiy N, Chen D, Gonugunta VK, Alto NM, Yan N (2015) STING activation by translocation from the ER is associated with infection and autoinflammatory disease. *Cell Host Microbe* 18: 157–168
- Ergun SL, Fernandez D, Weiss TM, Li L (2019) STING polymer structure reveals mechanisms for activation, hyperactivation, and inhibition. *Cell* 178: 290–301
- Furukawa Y, Fu R, Deng H-X, Siddique T, O'Halloran TV (2006) Disulfide cross-linked protein represents a significant fraction of ALS-associated Cu, Zn-superoxide dismutase aggregates in spinal cords of model mice. *Proc Natl Acad Sci USA* 103: 7148–7153
- Gao P, Ascano M, Zillinger T, Wang W, Dai P, Serganov AA, Gaffney BL, Shuman S, Jones RA, Deng L (2013) Structure-function analysis of STING activation by c[G(2', 5')pA(3', 5')p] and targeting by antiviral DMXAA. *Cell* 154: 748–762

- Gunderstofte C, Iversen MB, Peri S, Thielke A, Balachandran S, Holm CK, Olagnier D (2019) Nrf2 Negatively regulates Type I interferon responses and increases susceptibility to herpes genital infection in mice. *Front Immunol* 10: 2101
- Haag SM, Gulen MF, Reymond L, Gibelin A, Abrami L, Decout A, Heymann M, Van Der Goot FG, Turcatti G, Behrendt R (2018) Targeting STING with covalent small-molecule inhibitors. *Nature* 559: 269–273
- Holmström KM, Finkel T (2014) Cellular mechanisms and physiological consequences of redox-dependent signalling. *Nat Rev Mol Cell Biol* 15: 411–421
- Horner SM, Liu HM, Park HS, Briley J, Gale M Jr (2011) Mitochondrial-associated endoplasmic reticulum membranes (MAM) form innate immune synapses and are targeted by hepatitis C virus. *Proc Natl Acad Sci USA* 108: 14590–14595
- Hou F, Sun L, Zheng H, Skaug B, Jiang Q-X, Chen ZJ (2011) MAVS forms functional prion-like aggregates to activate and propagate antiviral innate immune response. *Cell* 146: 448–461
- Hu M-M, Yang Q, Xie X-Q, Liao C-Y, Lin H, Liu T-T, Yin L, Shu H-B (2016) Sumoylation promotes the stability of the DNA sensor cGAS and the adaptor STING to regulate the kinetics of response to DNA virus. *Immunity* 45: 555–569
- Huang Y-H, Liu X-Y, Du X-X, Jiang Z-F, Su X-D (2012) The structural basis for the sensing and binding of cyclic di-GMP by STING. *Nat Struct Mol Biol* 19: 728–730
- Ishikawa H, Barber GN (2008) STING is an endoplasmic reticulum adaptor that facilitates innate immune signalling. *Nature* 455: 674–678
- Ishikawa H, Ma Z, Barber GN (2009) STING regulates intracellular DNA-mediated, type I interferon-dependent innate immunity. *Nature* 461: 788–792
- Jin L, Lenz LL, Cambier JC (2010) Cellular reactive oxygen species inhibit MPYS induction of IFN $\beta$ . *PLoS One* 5: e15142
- Karbowski M, Neutzner A, Youle RJ (2007) The mitochondrial E3 ubiquitin ligase MARCH5 is required for Drp1 dependent mitochondrial division. *J Cell Biol* 178: 71–84
- Konno H, Konno K, Barber GN (2013) Cyclic dinucleotides trigger ULK1 (ATG1) phosphorylation of STING to prevent sustained innate immune signaling. *Cell* 155: 688–698
- Kranzusch PJ, Wilson SC, Lee AS, Berger JM, Doudna JA, Vance RE (2015) Ancient origin of cGAS-STING reveals mechanism of universal 2', 3' cGAMP signaling. *Mol Cell* 59: 891–903
- Kwon D, Park E, Kang SJ (2017a) Stimulator of IFN genes-mediated DNA-sensing pathway is suppressed by NLRP3 agonists and regulated by mitofusin 1 and TBC1D15, mitochondrial dynamics mediators. *FASEB J* 31: 4866–4878
- Kwon D, Park E, Sesaki H, Kang SJ (2017b) Carbonyl cyanide 3-chlorophenylhydrazone (CCCP) suppresses STING-mediated DNA sensing pathway through inducing mitochondrial fission. *Biochem Biophys Res Commun* 493: 737–743
- Kwon D, Sesaki H, Kang SJ (2018) Intracellular calcium is a rheostat for the STING signaling pathway. *Biochem Biophys Res Commun* 500: 497–503
- Li Z, Liu G, Sun L, Teng Y, Guo X, Jia J, Sha J, Yang X, Chen D, Sun Q (2015) PPM1A regulates antiviral signaling by antagonizing TBK1-mediated STING phosphorylation and aggregation. *PLoS Pathog* 11: e1004783
- Lin H, Li S, Shu H-B (2019) The membrane-associated MARCH E3 ligase family: emerging roles in immune regulation. *Front Immunol* 10: 1751
- Liu S, Cai X, Wu J, Cong Q, Chen X, Li T, Du F, Ren J, Wu YT, Grishin NV et al (2015) Phosphorylation of innate immune adaptor proteins MAVS, STING, and TRIF induces IRF3 activation. *Science* 347: aaa2630
- Liu S, Yang B, Hou Y, Cui K, Yang X, Li X, Chen L, Liu S, Zhang Z, Jia Y (2023) The mechanism of STING autoinhibition and activation. *Mol Cell* 83: 1502–1518
- Lu D, Shang G, Li J, Lu Y, Bai X-C, Zhang X (2022) Activation of STING by targeting a pocket in the transmembrane domain. *Nature* 604: 557–562
- Missiroli S, Patergnani S, Caroccia N, Pedriali G, Perrone M, Previali M, Wieckowski MR, Giorgi C (2018) Mitochondria-associated membranes (MAMs) and inflammation. *Cell Death Dis* 9: 329
- Mukai K, Konno H, Akiba T, Uemura T, Waguri S, Kobayashi T, Barber GN, Arai H, Taguchi T (2016) Activation of STING requires palmitoylation at the Golgi. *Nat Commun* 7: 11932
- Nagashima S, Takeda K, Ohno N, Ishido S, Aoki M, Saitoh Y, Takada T, Tokuyama T, Sugiura A, Fukuda T (2019) MITOL deletion in the brain impairs mitochondrial structure and ER tethering leading to oxidative stress. *Life Sci Alliance* 2: e201900308
- Nakamura N, Kimura Y, Tokuda M, Honda S, Hirose S (2006) MARCH-V is a novel mitofusin 2-and Drp1-binding protein able to change mitochondrial morphology. *EMBO Rep* 7: 1019–1022
- Ni G, Konno H, Barber GN (2017) Ubiquitination of STING at lysine 224 controls IRF3 activation. *Sci Immunol* 2: eaah7119
- Olagnier D, Brandtoft AM, Gunderstofte C, Villadsen NL, Krapp C, Thielke AL, Laustsen A, Peri S, Hansen AL, Bonefeld L (2018) Nrf2 negatively regulates STING indicating a link between antiviral sensing and metabolic reprogramming. *Nat Commun* 9: 3506
- Ouyang S, Song X, Wang Y, Ru H, Shaw N, Jiang Y, Niu F, Zhu Y, Qiu W, Parvatiyar K et al (2012) Structural analysis of the STING adaptor protein reveals a hydrophobic dimer interface and mode of cyclic di-GMP binding. *Immunity* 36: 1073–1086
- Park Y-Y, Cho H (2012) Mitofusin 1 is degraded at G 2/M phase through ubiquitylation by MARCH5. *Cell Div* 7: 25
- Park Y-Y, Lee S, Karbowski M, Neutzner A, Youle RJ, Cho H (2010) Loss of MARCH5 mitochondrial E3 ubiquitin ligase induces cellular senescence through dynamin-related protein 1 and mitofusin 1. *J Cell Sci* 123: 619–626
- Park YJ, Oanh NTK, Heo J, Kim SG, Lee HS, Lee H, Lee JH, Kang HC, Lim W, Yoo YS et al (2020) Dual targeting of RIG-I and MAVS by MARCH5 mitochondria ubiquitin ligase in innate immunity. *Cell Signal* 67: 109520
- Saitoh T, Fujita N, Hayashi T, Takahara K, Satoh T, Lee H, Matsunaga K, Kageyama S, Omori H, Noda T (2009) Atg9a controls dsDNA-driven dynamic translocation of STING and the innate immune response. *Proc Natl Acad Sci USA* 106: 20842–20846
- Serebryany E, Woodard JC, Adkar BV, Shabab M, King JA, Shakhnovich EI (2016) An internal disulfide locks a misfolded aggregation-prone intermediate in cataract-linked mutants of human gammaD-crystallin. *J Biol Chem* 291: 19172–19183
- Seth RB, Sun L, Ea C-K, Chen ZJ (2005) Identification and characterization of MAVS, a mitochondrial antiviral signaling protein that activates NF- $\kappa$ B and IRF3. *Cell* 122: 669–682
- Shang G, Zhu D, Li N, Zhang J, Zhu C, Lu D, Liu C, Yu Q, Zhao Y, Xu S et al (2012) Crystal structures of STING protein reveal basis for recognition of cyclic di-GMP. *Nat Struct Mol Biol* 19: 725–727
- Shang G, Zhang C, Chen ZJ, Bai XC, Zhang X (2019) Cryo-EM structures of STING reveal its mechanism of activation by cyclic GMP-AMP. *Nature* 567: 389–393
- Shi H-X, Liu X, Wang Q, Tang P-P, Liu X-Y, Shan Y-F, Wang C (2011) Mitochondrial ubiquitin ligase MARCH5 promotes TLR7 signaling by attenuating TANK action. *PLoS Pathog* 7: e1002057

- Shiiba I, Takeda K, Nagashima S, Yanagi S (2020) Overview of mitochondrial E3 ubiquitin ligase MITOL/MARCH5 from molecular mechanisms to diseases. *Int J Mol Sci* 21: 3781
- Shu C, Yi G, Watts T, Kao CC, Li P (2012) Structure of STING bound to cyclic di-GMP reveals the mechanism of cyclic dinucleotide recognition by the immune system. *Nat Struct Mol Biol* 19: 722–724
- Stetson DB, Medzhitov R (2006) Recognition of cytosolic DNA activates an IRF3-dependent innate immune response. *Immunity* 24: 93–103
- Subramanian N, Natarajan K, Clatworthy MR, Wang Z, Germain RN (2013) The adaptor MAVS promotes NLRP3 mitochondrial localization and inflammasome activation. *Cell* 153: 348–361
- Sugiura A, Nagashima S, Tokuyama T, Amo T, Matsuki Y, Ishido S, Kudo Y, McBride HM, Fukuda T, Matsushita N et al (2013) MITOL regulates endoplasmic reticulum-mitochondria contacts via Mitofusin2. *Mol Cell* 51: 20–34
- Sun W, Li Y, Chen L, Chen H, You F, Zhou X, Zhou Y, Zhai Z, Chen D, Jiang Z (2009) ERIS, an endoplasmic reticulum IFN stimulator, activates innate immune signaling through dimerization. *Proc Natl Acad Sci USA* 106: 8653–8658
- Sun L, Wu J, Du F, Chen X, Chen ZJ (2013) Cyclic GMP-AMP synthase is a cytosolic DNA sensor that activates the type I interferon pathway. *Science* 339: 786–791
- Tal MC, Sasai M, Lee HK, Yordy B, Shadel GS, Iwasaki A (2009) Absence of autophagy results in reactive oxygen species-dependent amplification of RLR signaling. *Proc Natl Acad Sci USA* 106: 2770–2775
- Tanaka Y, Chen ZJ (2012) STING specifies IRF3 phosphorylation by TBK1 in the cytosolic DNA signaling pathway. *Sci Signal* 5: ra20
- Tao L, Lemoff A, Wang G, Zarek C, Lowe A, Yan N, Reese TA (2020) Reactive oxygen species oxidize STING and suppress interferon production. *Elife* 9: e57837
- Toichi K, Yamanaka K, Furukawa Y (2013) Disulfide scrambling describes the oligomer formation of superoxide dismutase (SOD1) proteins in the familial form of amyotrophic lateral sclerosis. *J Biol Chem* 288: 4970–4980
- Tsuchida T, Zou J, Saitoh T, Kumar H, Abe T, Matsuura Y, Kawai T, Akira S (2010) The ubiquitin ligase TRIM56 regulates innate immune responses to intracellular double-stranded DNA. *Immunity* 33: 765–776
- van Dam L, Dansen TB (2020) Cross-talk between redox signalling and protein aggregation. *Biochem Soc Trans* 48: 379–397
- Wang Q, Liu X, Cui Y, Tang Y, Chen W, Li S, Yu H, Pan Y, Wang C (2014) The E3 ubiquitin ligase AMFR and INSIG1 bridge the activation of TBK1 kinase by modifying the adaptor STING. *Immunity* 41: 919–933
- Wang Y, Lian Q, Yang B, Yan S, Zhou H, He L, Lin G, Lian Z, Jiang Z, Sun B (2015) TRIM30 $\alpha$  is a negative-feedback regulator of the intracellular DNA and DNA virus-triggered response by targeting STING. *PLoS Pathog* 11: e1005012
- Weinberg SE, Sena LA, Chandel NS (2015) Mitochondria in the regulation of innate and adaptive immunity. *Immunity* 42: 406–417
- Xing J, Zhang A, Zhang H, Wang J, Li XC, Zeng M-S, Zhang Z (2017) TRIM29 promotes DNA virus infections by inhibiting innate immune response. *Nat Commun* 8: 945
- Xu S, Cherok E, Das S, Li S, Roelofs BA, Ge SX, Polster BM, Boyman L, Lederer WJ, Wang C (2016) Mitochondrial E3 ubiquitin ligase MARCH5 controls mitochondrial fission and cell sensitivity to stress-induced apoptosis through regulation of MiD49 protein. *Mol Biol Cell* 27: 349–359
- Ye L, Zhang Q, Liuyu T, Xu Z, Zhang M-X, Luo M-H, Zeng W-B, Zhu Q, Lin D, Zhong B (2019) USP49 negatively regulates cellular antiviral responses via deconjugating K63-linked ubiquitination of MITA. *PLoS Pathog* 15: e1007680
- Yin Q, Tian Y, Kabaleeswaran V, Jiang X, Tu D, Eck MJ, Chen ZJ, Wu H (2012) Cyclic di-GMP sensing via the innate immune signaling protein STING. *Mol Cell* 46: 735–745
- Yonashiro R, Ishido S, Kyo S, Fukuda T, Goto E, Matsuki Y, Ohmura-Hoshino M, Sada K, Hotta H, Yamamura H (2006) A novel mitochondrial ubiquitin ligase plays a critical role in mitochondrial dynamics. *EMBO J* 25: 3618–3626
- Yoo YS, Park YY, Kim JH, Cho H, Kim SH, Lee HS, Kim TH, Sun Kim Y, Lee Y, Kim CJ et al (2015) The mitochondrial ubiquitin ligase MARCH5 resolves MAVS aggregates during antiviral signalling. *Nat Commun* 6: 7910
- Zamorano Cuervo N, Fortin A, Caron E, Chartier S, Grandvaux N (2021) Pinpointing cysteine oxidation sites by high-resolution proteomics reveals a mechanism of redox-dependent inhibition of human STING. *Sci Signal* 14: eaaw4673
- Zhang J, Hu M-M, Wang Y-Y, Shu H-B (2012) TRIM32 protein modulates type I interferon induction and cellular antiviral response by targeting MITA/STING protein for K63-linked ubiquitination. *J Biol Chem* 287: 28646–28655
- Zhang X, Shi H, Wu J, Zhang X, Sun L, Chen C, Chen ZJ (2013) Cyclic GMP-AMP containing mixed phosphodiester linkages is an endogenous high-affinity ligand for STING. *Mol Cell* 51: 226–235
- Zhang M, Zhang M-X, Zhang Q, Zhu G-F, Yuan L, Zhang D-E, Zhu Q, Yao J, Shu H-B, Zhong B (2016) USP18 recruits USP20 to promote innate antiviral response through deubiquitinating STING/MITA. *Cell Res* 26: 1302–1319
- Zhang L, Wei N, Cui Y, Hong Z, Liu X, Wang Q, Li S, Liu H, Yu H, Cai Y (2018) The deubiquitinase CYLD is a specific checkpoint of the STING antiviral signaling pathway. *PLoS Pathog* 14: e1007435
- Zhang C, Shang G, Gui X, Zhang X, Bai XC, Chen ZJ (2019) Structural basis of STING binding with and phosphorylation by TBK1. *Nature* 567: 394–398
- Zhong B, Yang Y, Li S, Wang YY, Li Y, Diao F, Lei C, He X, Zhang L, Tien P et al (2008) The adaptor protein MITA links virus-sensing receptors to IRF3 transcription factor activation. *Immunity* 29: 538–550
- Zhong B, Zhang L, Lei C, Li Y, Mao A-P, Yang Y, Wang Y-Y, Zhang X-L, Shu H-B (2009) The ubiquitin ligase RNF5 regulates antiviral responses by mediating degradation of the adaptor protein MITA. *Immunity* 30: 397–407
- Zhou R, Tardivel A, Thorens B, Choi I, Tschopp J (2010) Thioredoxin-interacting protein links oxidative stress to inflammasome activation. *Nat Immunol* 11: 136–140
- Zhou R, Yazdi AS, Menu P, Tschopp J (2011) A role for mitochondria in NLRP3 inflammasome activation. *Nature* 469: 221–225